CHESTER

Compressed Heat Energy
Storage for Energy
from Renewable sources

Advanced dynamic model for full scale CHEST system integration into energy networks

PROJECT	**CHESTER**
PROJECT NO.	**764042**
DELIVERABLE NO.	**D4.2**
DOCUMENT VERSION	**V2.0**
DOCUMENT PREPARATION DATE	**28-09-2021**
RESPONSIBILE PARTNER	**AIGUASOL**
DISSEMINATION LEVEL	**PUBLIC**

Type of Deliverable		
R	Document, Report	x
DEM	Demonstrator, pilot, prototype	
DEC	Websites, patent fillings, videos, etc.	
OTHER		
ETHICS	Ethics requirements	
ORDP	Open Research Data Pilot	

This project has received funding from the European Union's Horizon 2020 research and innovation programme under grant agreement No. 764042.

This deliverable reflects only the author's views and neither Agency nor the Commission are responsible for any use that may be made of the information contained therein.

EC Grant Agreement	No.764042
Project Acronym	CHESTER
Project Title	Compressed Heat Energy Storage for Energy from Renewable sources
Programme	HORIZON 2020
Start Date of Project	01-04-2018
Duration	48 Months

Financial/Administrative Coordinator	
Project Coordinator Organization Name	TECNALIA
Address	Parque Tecnológico de Bizkaia C/Astondo, Edificio 700 (Spain)
Phone Numbers	+34 946 430 850
E-mail Address	nora.fernandez@tecnalia.com
Project web-site	www.chester-project.eu

Version Management			
Filename		D4.2: Advanced dynamic model for full scale integration of the CHEST system into energy networks	
Author(s)		AIGUASOL	
Reviewed by		[Name]	
Approved by		[Name]	
Revision No.	**Date**	**Author**	**Modification description**
RV 1	21/10/22019	S. Stark, D. Bestenlehner	Review of the deliverable
RV 2	5/11/2019	A. Carrera	Incorporate comments from review, added section 4.5 describing outputs.
RV 3	10/11/2019	S. Ochoa de Eribe	Review of the 3.1, 3.2, 3.3 sections
RV 4	11/11/2019	S. Amelio	Review of the 3.1, 3.2, 3.3 sections
RV 5	12/11/2019	S. Lecompte	Review of section 4.6
RV 6	14/11/2019	F. Bava	Review of the overall text and format
RV 7	15/11/2019	T. Weller	Review of section 4.5 and 4.7
RV 8	18/11/2019	Tecnalia	Review of section 4.3 and overall text
RV 9	28/09/2021	A. Carrera	Incorporate comments from PO review.

Contents

List of Figures

List of Tables

Glossary, abbreviations and acronyms

CAES	Compressed Air Energy Storage
CHEST	Compressed Heat Energy Storage
COP	Coefficient of Performance
DAM	Day Ahead Market
DSO	Distribution System Operator
EES	Electrical Energy Storage
ENTSOE	European Network of Transmission System Operators for Electricity
FCR	Frequency Containment Reserve
FRR	Frequency Restoration Reserve
GA	Grant Agreeement
HTF	Heat transfer fluid
HP	Heat pump
HTWT	Hot Temperature Water Tank

HVAC	Heating Ventilation and Air Conditioning
HX	Heat Exchanger
IPP	Independent Power Producer
LTWT	Low Temperature Water Tank
NEMO	Nominated Electricity Market Operator
PHS	Pumped hydro storage
ORC	Organic Rankine Cycle
OTC	Over the Counter
PCM	Phase Change Material
PPA	Power Purchase Agreement
PV	Photovoltaic
RR	Replacement Reserve
SHS	Sensible heat storage
TSO	Transmission System Operator
UA	Heat transfer coefficient multiplied by the area

1. Executive Summary

This document describes the work carried out in the T4.2 of the CHESTER project. The aim of the task is to develop an advanced dynamic model of the CHEST system and its integration into the energy system. This integration is relevant since it identifies additional requirements/constraints of the system that shall be addressed in the development of the technology to become a commercial alternative.

In the work done, the first step has been to establish the format of such market integration. Electrical storage is a grid service that has benefits on several aspects of the liberalized market: at generation level (reserve capacity), transmission level (investment deferral), distribution level (voltage control) and customer level (peak shaving). Historically, it was controlled by the monopolistic companies ruling the market prior liberalization, but nowadays, with the valorization of these benefits split across the different activities of the liberalized electricity sector, the monetarization of the benefits of electricity storage is far more difficult. Moreover, the legal situation is ambiguous, also due to the contradictions posed on one side by the integral role of the storage in the electricity grid and on the other the liberalization of the different market sectors (distribution, transmission and generation). As far as the integration of the CHEST system is concerned, we assume that the correct integration of the CHEST system in the future electrical market will be in the form of reserve capacity at generation level. Accordingly, from the electrical market analysis presented, a sequential multi-market strategy is selected, meaning that the CHEST system operates simultaneously in at least two electrical markets: the reserve market, which is the market mechanism where the electricity storage fits best and gets maximum revenues, but also, on the day-ahead market. Besides, specific technical requirements imposed by the market rules have been identified, albeit relaxed, due to the tendencies of the legal framework regarding the electrical balancing market rules.

Once this integration has been established, the task work has been focused on the development of the model to optimize the mentioned operational strategy. Following the GA requirements, the model is dynamic, meaning that the transient operation of the system is taken into account. In the modelling work, the main effort has been devoted to the characterization of the interaction between the PCM storage and both the ORC turbine and the heat pump. This is motivated by the thermal dynamics of this integration, that, as explained in the document, is quite different to the usual condenser/evaporator control management in conventional ORC/HP applications. Besides, the aim has been to keep always the model as simple as possible, and keep the effort on modelling the most uncertain heat transfer phenomena in the system., which is the heat transfer at the PCM. To model the CHEST system in TRNSYS, a set of component models had to be programmed, and they are documented and available for future use in the project. Also, a coupling with the refrigerant properties database CoolProp has been programmed to improve the model capabilities. Finally, the whole system model consisting in more than 60 components was programmed.

With this work of theoretically upscaling the CHEST system to the context of the electrical market, several relevant conclusions have been drawn, regarding both operational and technical aspects of the system that need to be addressed in the system development.

2. Introduction

2.1. Purpose and Scope

The present document describes the advanced dynamic model of the CHEST system developed within T4.2. The aim of the model is to assess the potential of the CHEST system within the electrical market, as well as becoming a main input to task 4.4.

Inherently to the task objectives, there is the need to define an exploitation route of the system, since the electrical market itself is a set of different markets where not only electricity, but also other services needed for the proper operation of the electricity grid are exchanged in a very dynamic context. As the main potential of the CHEST system is to work as an electricity storage system in an upcoming future of the electrical grid characterized by a huge increase of non-dispatchable electricity sources (renewables), the basis of this exploitation of the system is mirrored in the business model of the Pumped Hydro Storage (PHS) systems.

2.2. Structure of the document

The document is structured in two main parts. The first, section 3, analyses how the CHEST model can be introduced in the electrical market under the current legal framework and what is the market structure of the electrical storage in the electrical market and what operational strategies are followed. This is necessary since the current electrical market is in practice a set of sequential markets rather than a single pool market, and the role of CHEST in the electrical system will need to be optimized in that context. The boundary conditions imposed to the system are listed and relaxed in view of the presented tendencies of the regulatory framework, [1] which is actually very dynamic due to the standardization efforts of the electrical market taken by the European Commission.

The second, section 4, describes the model developed in T4.2 to characterize the system performance in the T4.4. The aim there is to establish an optimized operation strategy of the system in real time. This section is mostly a documental work in order to allow users of the model the understanding of the results and the correct parameterization of the use for the future uses of it in the CHEST project.

Finally, the section 5 contains the conclusions derived from the presented work

3. Introduction of CHEST in the electricity market

3.1. Overview of the electricity market

As noted previously, one of the objectives of the T4.2 is modelling the performance of the CHEST system integrated in the electrical grid. In this section, we make an overview of the electricity market, as a preliminary introduction to the role and associated constraints of the CHEST system in the electrical system.

The current design of the electricity markets is the result of a long-term legislative effort by the EU that begins on the 1990s, where the liberalization of the national markets dominated by the old monopolies over generation, transmission and distribution started. Nowadays, a fully integrated internal electricity market is one of the five dimensions of the European Commission energy strategy, known as the Energy Union strategy, published on February 2015. Since then, the European Commission has launched several legislative packages that address the objectives of the Energy Union strategy, including the integrated electricity market. Although the deployment of this electricity market is not finished, this integration effort has yielded a very similar structure of the electricity market in all the EU countries.

Electricity is a product characterized by the property that the consumption and generation must be the same at every moment. Otherwise, the network frequency deviates from its setpoint value and the system destabilizes, eventually collapsing. Due to this particularity, the electricity market consists, rather than on a single market, on a set of sequential markets where consumers and generators agree on electricity exchanges at different time horizons. The electricity can be exchanged from years before consumption to the same hour where it is consumed, and depending on the timeframe, these exchanges take place on different markets. Figure 1 shows a scheme of the different markets that conform the electricity market:

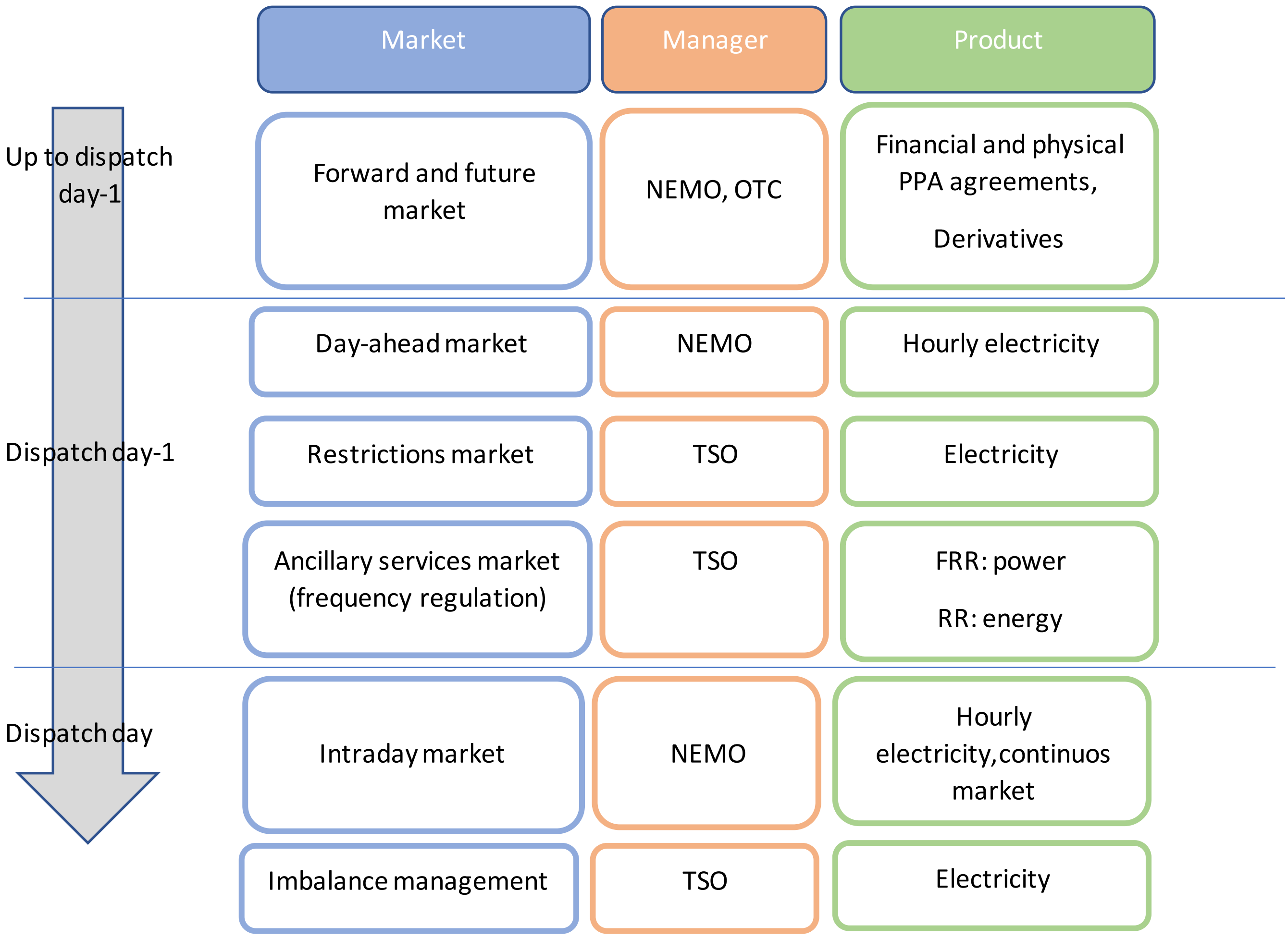

Figure 1: Schematic overview of electricity market

We will make a short description of the different markets shown in figure 1.

a. The **forward and futures market** are bilateral contracts between producers and consumers to purchase a certain amount of electricity in a specified quantity and period. Usually forward contracts imply a physical exchange of electricity between producers and consumers and the terms are agreed between the parts, while future markets are a standardized product organized by a Market Operator that can be further traded or exchanged.
b. The **day-ahead market (DAM) takes** place the day before the dispatch of electricity, and the generators and distributors/consumers deliver proposals to the Market Operator for the 24 hours of the next day. The Market Operator is responsible of balancing generation and consumption in their zone, and based on this schedule for the operation of the energy generators for the next day. The day-ahead market is the fundamental piece of the electricity market, since it holds most of the electricity exchanges that take place.
c. The **restrictions market** is managed by the TSO and takes place after the day-ahead market. It is not a proper market, in the sense that no offers are made, rather, it is the correction of the day-ahead market results due to technical limitations of the distribution grid (mainly, the inability of the grid to deliver the DAM results due to grid capacity).
d. The **ancillary services** market is a set of markets where different products needed for the proper operation of the system are offered. Most relevant among them is the balancing market, where participants offer resources to the TSO to balance the electrical grid in the event that the predicted consumption and generation differ. This happens for instance, when a generating plant suffers technical problem, or when forecasted production by renewable energy differs from the real-time production. In section 3.3 we give further insight on the structure of this market.
e. The **intra-day market** takes place the same day as the electricity is dispatched, and thanks to this, allows for a better forecasting of their portfolio to the generators and consumers. This is a relevant market specially for those generators that rely on renewable energy sources since the forecast of their production improves compared to the forecast done the day before. After here, the Market Operator has balanced the production and generation within a few hours of the dispatch of electricity, and the TSO is responsible for the proper operation of the system.

   The European market is evolving to a homogeneous bidding system. Probably, nowadays, continuous means ‘hourly’ but in other countries may be is a 15 minutes market or less time.

f. The **management of imbalances** is not a proper market, instead is a well-defined technical procedure to ensure in real-time that the electrical system is balanced. However, it is also the procedure through which part of the ancillary markets monetize their participation in the electricity market. According to the evolution of the grid in operation, the TSO calls to market participants to deliver services, which have been selected according to the balancing market that took place the day ahead.

Any participant of the electrical market has to offer services within the presented scheme, and in order to participate in any segment, it is necessary to meet specific technical conditions. Thus, in the process of modelling the CHEST system integrated into the energy networks it is necessary to identify a role for it in the electricity market. It is important to note that in general not all the markets are mandatory: in particular, participation in the reserve capacity market does not mean the obligation of participating in the DAM market, although to participate in the intraday market it is necessary to have send priory an offer to the DAM market. Since the CHEST is an electricity storage device, we will see in the next section how the state-of-the-art technologies of electricity storage participate in the market to define the economic model for CHEST.

3.2. Storage on the electricity market

3.2.1. Regulatory framework

The lack of regulatory framework for the energy storage is a frequent conclusion on the analysis of the electricity storage situation in Europe [2]. Main factor is the unbundling of the activities in the electricity sector (generation, distribution, transmission) encouraged by the EU in the last decades, since the benefits of electrical storage are in general distributed between several stakeholders in the electricity sector. According to DG Energy, this includes [3]:

- Generation level: Arbitrage, balancing and reserve power, etc.
- Transmission level: frequency control, investment deferral
- Distribution level: voltage control, capacity support, etc.
- Customer level: peak shaving, time of use cost management, etc.

The value proposition thus gets distributed between unbundling activities, and often a single one of the benefits cannot account for a viable business model [4] [5].

Due to the lack of regulation at EU level energy storage faces a variety of frameworks at national level in the EU [6]. There is no consistency amongst the Member States on the way storage is treated in the energy system. For instance, in several countries storage facilities pay grid fees both as consumer and producer, in other countries only as producer, or they have other special regimes.

This has been addressed by the European Parliament in the recent (June 2019) Directive [7] on common rules for the internal market for electricity, establishing common rules for storage. This directive sets a definition of electrical storage: “energy storage” means, in the electricity system, deferring the final use of electricity to a moment later than when it was generated, or the conversion of electrical energy into a form of energy which can be stored, the storing of such energy, and the subsequent reconversion of such energy into electrical energy or use as another energy carrier.

The directive also explicitly prohibits the DSO or TSO to own, manage or operate electricity storage “except when they are used for the sole purpose of ensuring a secure and reliable operation of the transmission or distribution system, and not for balancing or congestion management” and the regulatory authority has granted his approval.

Regarding the ownership of the storage the Directive establishes that “in the new electricity market design, energy storage services should be market-based and competitive. Consequently, cross-subsidisation between energy storage and the regulated functions of distribution or transmission should be avoided".

The deadline for the transposition of this Directive to the national level should take place before 1/1/2021, and since it was published 2 months before the generation of this deliverable, it is not yet possible to clarify how the situation of the storage will evolve in regulatory terms. However, the Directive foresees two different exploitation routes in the future:

1. As a network component used to ensure reliable operation of the system by the TSO/DSO whenever no third parties are in condition to deliver such services following a transparent tendering process
2. As market based services open to all market participants

3.2.2. Current status of electrical storage in the electricity market

Besides the lack of a homogeneous regulatory framework at European level, and the contradictions that appear in some countries regulations, the electrical storage is present in all European countries and has a relevant role in the proper operation of the system.

Pumped-hydro storage (PHS) is the main technology used to provide electricity storage services in the grid. Along with Compressed Air Energy Storage (CAES), it is at present the only storage technology capable of cost-effectively storing large amounts of electricity (terawatt-hours) over multiple days [8]. Japan (26 GW), China (23 GW), and the US (20 GW) have the highest installed capacity for pumped-hydro storage. The figure 2, taken from [8], shows the distribution of technologies operating worldwide as electricity storage, and PHS represents over 99 % of total global capacity.

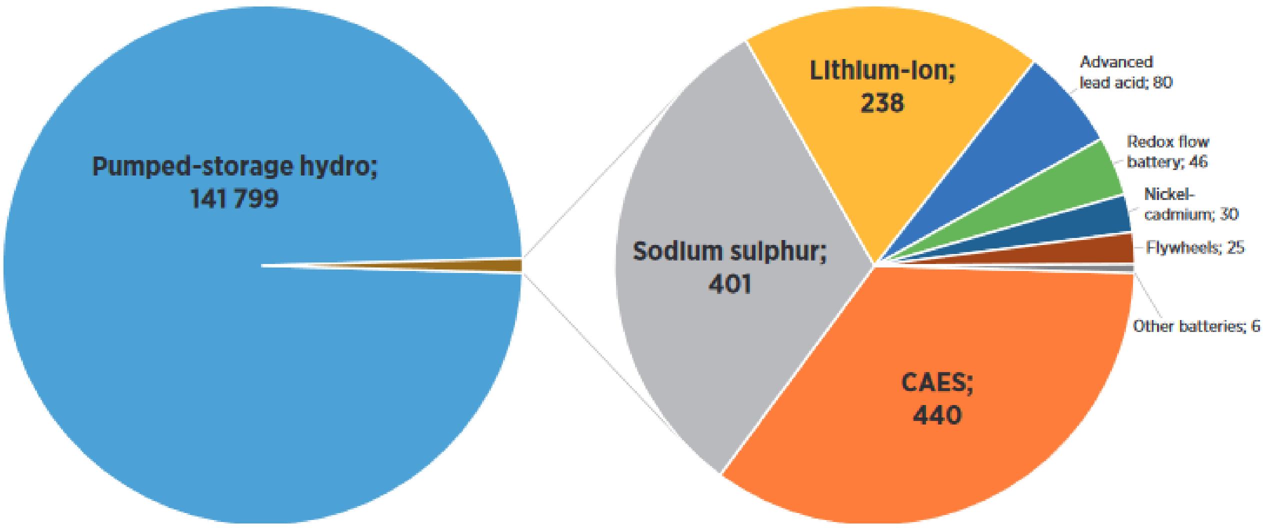

Figure 2: Share of pumped-hydro storage hydroelectricity in global electricity storage system [8], data in MW

Regarding the participation of the EES in Europe, the situation is very similar to the global tendencies. According to [4], by 2016, there were approximately 49 GW of storage deployed in the EU28. Figure 3 [4] shows the distribution of technologies in Europe.

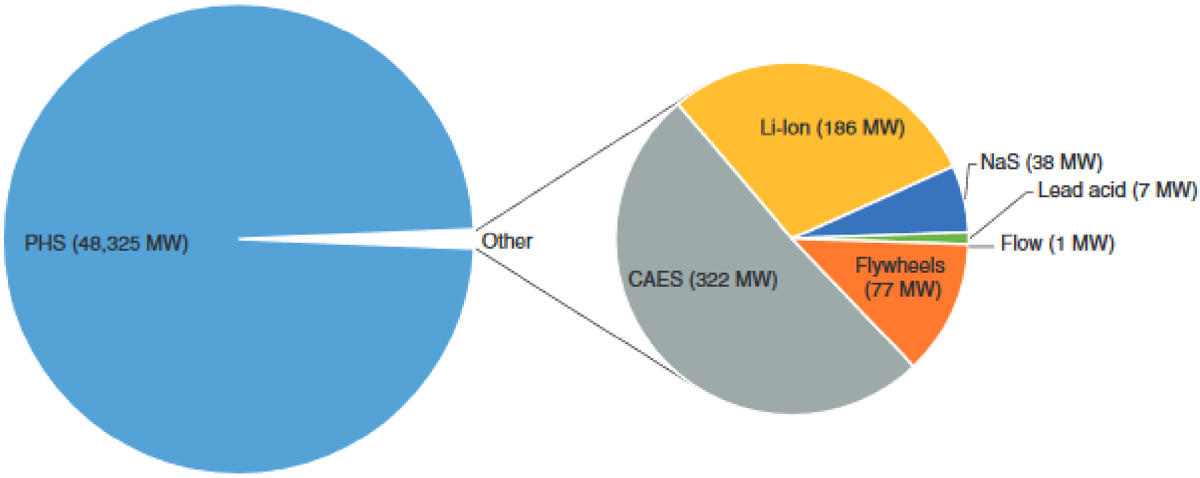

Figure 3: Share of pumped-hydro storage hydroelectricity in EU28+Norway+Switzerland electricity storage [4]

Hence, the current status of applications of the PHS is considered a good reference of an exploitation route of the CHEST system within the electricity market, since both show similar technical characteristics and services to be offered. Both technologies, as well as CAES, show a power capacity in the range of tens or hundreds of MW, maintaining operation during hours [4], while other EES technologies like batteries or flywheels show capacity ranging in a few MW, and duration from seconds to hours.

However, the reference of PHS is not straightforward, mainly because most of the installed capacity has been deployed during the 20th century under very different market structures. The figure 4, taken from [9], shows the commissioning of the worldwide capacity according to the market structure where it was developed:

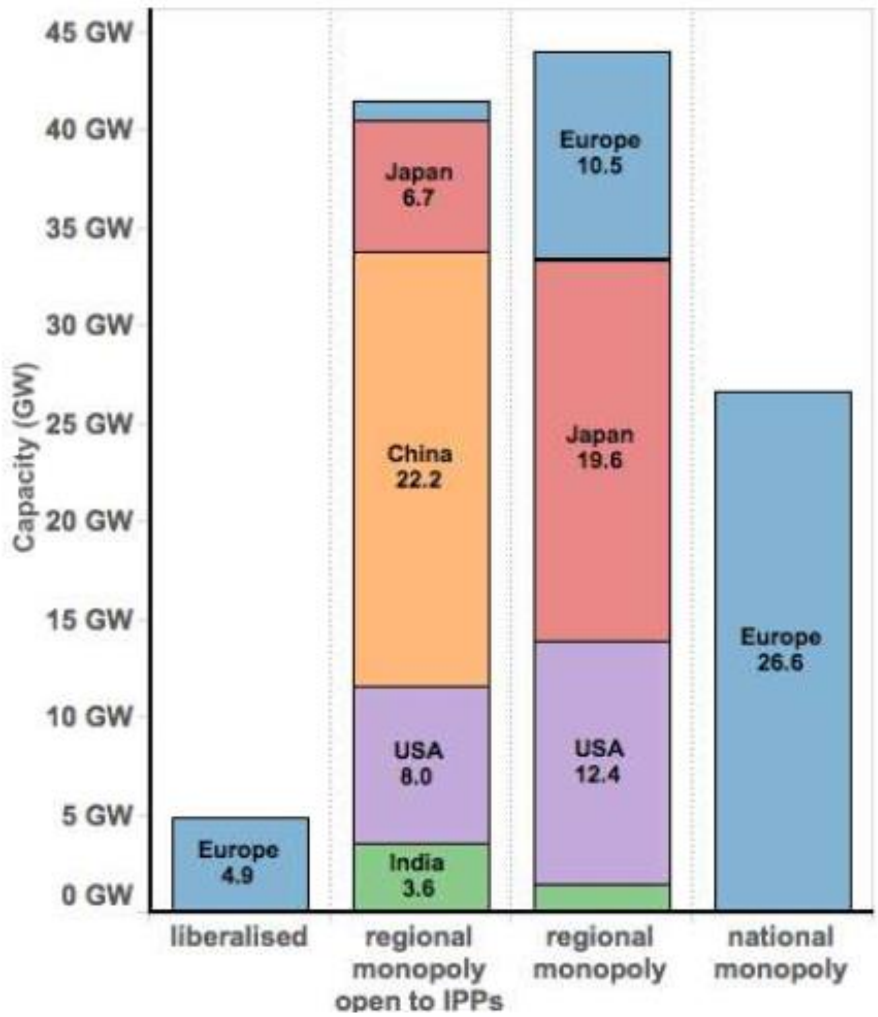

Figure 4: Capacity (GW) of PHS commissioned under different market structures [9]

It is worth to point out that less than 5 % of the analyzed capacity was deployed under a liberalized market structure. Under the regulated market structures that foster the deployment of the storage, the multiple benefits of the EES could be capitalized by the utility company, and the operation of the asset could be done in a much simpler fashion, since prices and production were far more predictable and the system costs were centralized. The traditional operation status of PHS aimed at reducing operating costs of the system by means of peak shaving, but also to offer ancillary services like maintaining power quality, voltage or frequency and providing reserves in case of emergency [10].

With the onset of the liberalized market, the peak shifting capacity of electrical storage has to be allocated in the different sequential markets described in section 3.1. Several researches have shown that the traditional operation based on peak shaving can be hardly profitable or even a loss [11]. Due to this, in the past years, several publications have proposed the PHS to participate in other markets and services, apart from the day-ahead energy market, in order to enlarge their income: in the secondary regulation service, in tertiary regulation services and intraday market. As it was noted in [12], and [13], among others, the revenues that a PHS can obtain from providing ancillary services are of a pretty considerable magnitude in comparison with those that can be obtained from levelling the power demand. Overall, the trends in the operation of PHS can be summarized as follow [14]:

- Day-ahead market operation is no longer profitable
- Reserve market is an important source of revenue in the liberalized market context
- Great effort is being done in the forecasting of day-ahead, intra-day and reserve market prices, since the uncertainty in the knowledge of the future values hampers the optimal operation and scheduling of the system
- Strategic bidding in sequential electricity markets is the operation strategy which allows for return of the investment in new developments

Based on this literature survey, the proposed strategy for the economic model of the CHEST system assumes a strategy based on bidding on the day-ahead market as well as the reserve market capacity. The approach ignores the possibility of operating into the intra-day market, due to the following reasons:

- Volume traded in the day-ahead market is substantially higher than the volume traded in the intra-day market
- Prices of both markets are strongly correlated, so it is considered that the economic revenue would slightly increase at the cost of a more complex system and a higher uncertainty in the optimization of the operation strategy

The assumption of operating in two markets means also that additional technical constraints must be fulfilled by the system in order to participate in each of them. Being the reserve market a much more stringent technical environment, in the next section we will describe the technical constraints imposed by the reserve market.

3.3. The balancing market rules

The Commission Regulation 2017/2195 [15] of 23 November 2017 establishing a guideline on electricity balancing lays down detailed rules for the integration of balancing energy markets in Europe, with the objectives of fostering effective competition, non-discrimination, transparency and integration in electricity balancing markets, and by doing so, enhancing the efficiency of the European balancing system as well as security of supply. It foresees the implementation of platforms at European level to exchange the resources of the different balancing markets, hence enforcing harmonization of products and processes at European level. The full deployment of the platforms should be finished by 2022.

European TSOs use different solutions to balance the system and restore the frequency, based on historic developments, but balancing energy in Europe is now organized into four steps:

- Frequency containment reserve
- Imbalance netting
- Frequency restoration reserves (automated or manual)
- Replacement reserve

From these steps, the imbalance netting is not organized into a market, since it is an operational procedure among geographically linked TSOs to correct their frequency when their frequency deviation is of opposite sign. The rest are standardized products that are called on sequentially as shown in the figure 5:

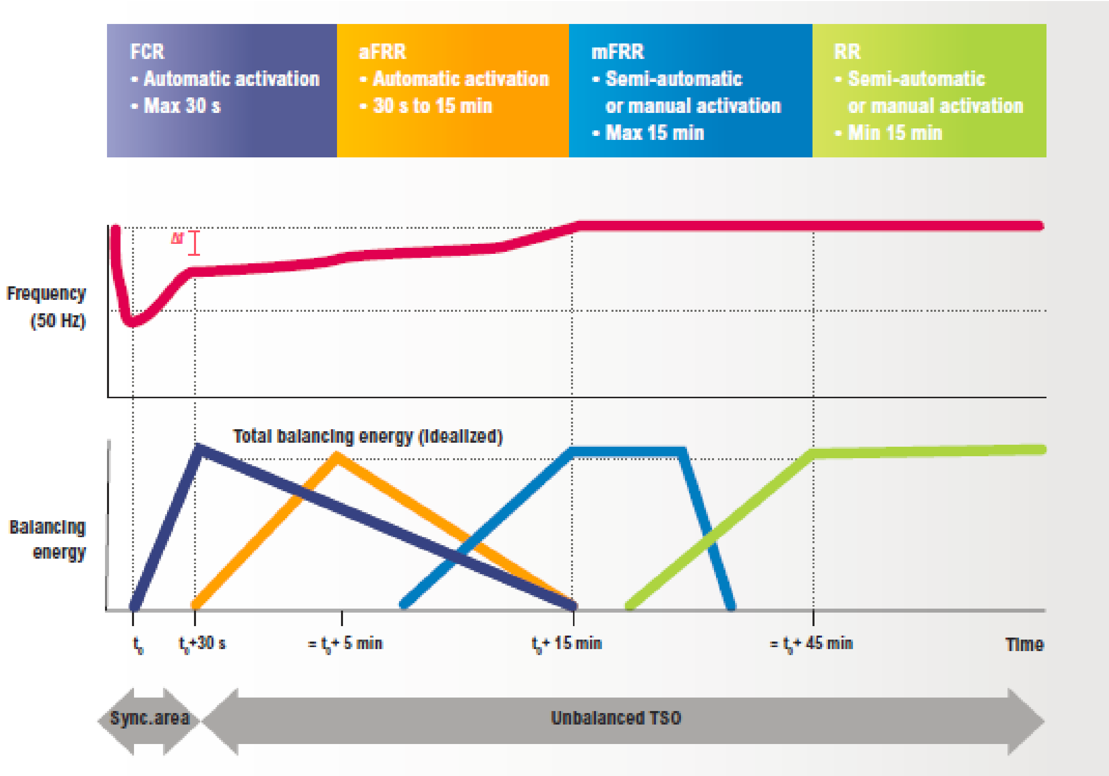

Figure 5: Balancing market products [1]

The event that triggers the activation of reserves is a deviation in the frequency of the electrical grid over the tolerance. After then, the different reserves are activated sequentially:

1. First, the Frequency Containment Reserve (FCR) activates his capacity immediately driving frequency to a stable value within his acceptable change. The time to reach full capacity for the FCR products cannot exceed 30 seconds from the triggering event, so they respond automatically to the network state. Traditionally this has been known as Primary Control. Not all the national systems have a proper FCR market, in some cases, like Spain or Italy, the power generators have to provide this service, while in others like Germany or France, there exists a proper market for tendering this service.
2. Within a few minutes, between 5 or 15, from the activation of the FCR, the Frequency Restoration Reserves (FRR) are activated. The automatic reserves are activated automatically by the TSO, while the manuals are called on upon request from the TSO. The objective of this reserve is to return the frequency to the nominal value. The traditional classification of the ENTSOE Operation Handbook calls the automatic reserve as secondary control, while the semi-automated or manual lie in the tertiary control [16]. Usually, secondary control is remunerated based on capacity provided independently of the activation of the reserves, while tertiary control is remunerated only when they are requested to deliver energy to the grid, not per availability.
3. Finally, from 15 minutes and more from the event, the Replacement Reserves are activated. The role of this reserve is to free the FRR so they are available in the case that another imbalance event appears. As tertiary control, they are often remunerated per energy basis.

To allow for a fast exchange of information and maximize the economic efficiency of the process, the directive 2017/2195 sets standardization of these products that are to be exchanged in the reserve market. To this end, it lists certain requirements for the technical parameters of the standard products:

1. Preparation period
2. Ramping period
3. Full activation time
4. Minimum and maximum quantity
5. Deactivation period
6. Minimum and maximum duration of delivery period
7. Validity period
8. Mode of activation

The figure 6, taken from [1], shows graphically the interpretation of most of these parameters:

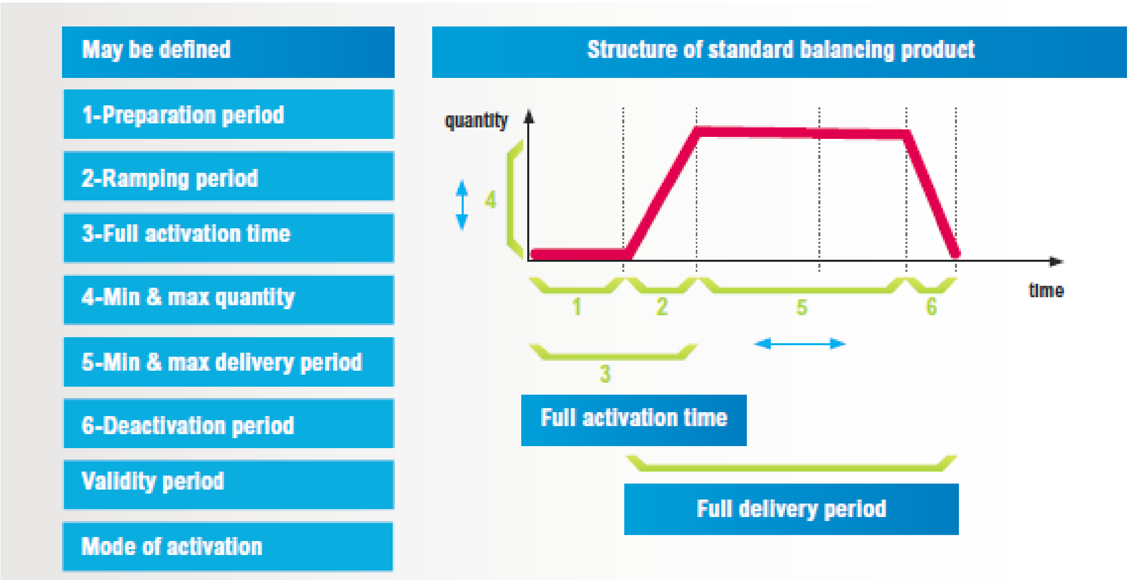

Figure 6: Structure of standard balancing product according to EU Directive 2017/2195 [1]

The current national balancing markets have strong differences in design, among other, on the acceptable limits to the quantities of the standard products that can be exchanged. The traditional markets are currently standardized in terms of Primary Control (FCR in the EU directive 2017/2195), Secondary Control (aFRR) and Tertiary control (mFRR and RR).

In the next table, that compiles data taken from [17, 18], we show the current characteristics of the balancing markets that are relevant in the design and sizing of the CHEST system. Many countries are missing since they lack a balancing market that defines the standard products in the same terms of the EU directive, or lack equivalent markets:

Table 1: Properties of balancing markets products in some EU countries

Country	Secondary Reserve minimum bid	Secondary Reserve activation time	Tertiary Reserve minimum bid	Tertiary Reserve activation time	Tertiary Reserve duration time
Austria	1 MW (symmetric)	300 s	1 MW		4 h
Denmark	1 MW	5 min (est DK) 15 min (west DK)	5 MW	15 min	30 min
Finland	5 MW	2 min	5 MW	60 min	
France	No market	No market	10 MW	15 min	
Germany	5 MW	5 min	5 MW	15 min	4 h
Hungary	1 MW	15 min	1 MW	15 min	
Netherlands	1 MW	15 min	20 MW		
Spain	10 MW	5 min	10 MW	15 min	2 h

From the CHEST design point of view, all these parameters are of consideration if the system has to be operated under a strategy of bidding in the reserve capacity together with DAM, which seems necessary according to the scientific literature to maximize benefits. The minimum quantity is the power required to be absorbed by the compressor, and also the minimum power of the ORC turbine. Also, the delivery period sets the minimum capacity that the latent storage of the CHEST system has to hold in order to meet the requirements. In some countries, like Austria, the up and down regulation has to be symmetric, which in terms of the CHEST system, means to have the same size for the HP and the ORC turbine

3.4. Summary of boundary conditions of the market in the CHEST sizing and operation

To summarize this section, we conclude the following points:

First, according to the operational strategy of technologies with a comparable performance and role in the electricity sector, the optimization of the CHEST system into the energy system requires the participation in the reserves capacity market, as well as the best known and commonly used day-ahead market. According to the referenced scientific literature, the revenues associated for the electrical storage systems are far bigger in the reserves capacity market, but the opportunities posed by the day-ahead market and the intra-day market should be exploited to maximize use. This will be the context in which the optimization strategy of T4.4 will be performed.

Second, the participation in these markets implies the fulfilment of several conditions in technical terms as capacity or response time, and these conditions vary widely among European countries. As presented previously, this is motivated mainly by historical reasons, but the current trend is the standardization at European level of the reserve markets as a prerequisite for the liberalization of the reserve markets as has been already done with the day-ahead market. Among these tendencies, there is one to reduce the required system capacity to facilitate the incorporation of demand response solutions, batteries and renewable energy technologies in the market. Due to this, we will consider that the minimum capacity requirements in the present scenario will no longer hold in the future, and that the minimum CHEST system capacity will be standardized at European level at 1 MW. However, the restrictions on response time will be maintained since this has already been set by a recent Directive from June 2019 and they are basic constraints of the ORC turbine and the heat pump systems, which require a minimum start up time. Based on the feedback by the consortium partners developing the technologies, we assume a start-up time for the HP of 5 minutes and 15 minutes for the ORC.

Related to the network requirements, it is important to note that the control of the CHEST system itself has to be defined in such a way that power input and output is controllable, in order to allow that the system can match the market bidding strategy. As we show in the next section, this will have implications in the selection of refrigerants and the temperature levels of the CHEST system.

4. Model description

4.1. CHEST scenarios and case studies

In previous work done in WP2, two among the seven case studies included in the project were selected as target for further optimization within WP4. The reader can refer to D2.1, where the description of the seven case studies, and in particular the two concerning WP4, is included.

The two case studies selected are Aalborg located in Denmark and Ispaster located in Spain; those are being either monitored or operational data from previous years are available, and information recovered in the monitoring platform developed in T4.1. This information, together with the model described in the present document, will become the pillars of the optimization task foreseen for T4.4.

The case study of Aalborg is centred around the local DH network in the city of Aalborg. The system has a heat demand in the range of 2000 GWh/year, and several sources of excess heat connected that can help the integration of the CHEST system. In this case study, the CHEST system operates as an electrical storage device for the electrical grid, coupled to the DH system, and the external controlling signals are based on the market prices. This will correspond to a situation that the system gets revenues by offering grid services.

The case study of Ispaster is completely different, since it is a small micro grid and no connection to a market can be considered; here the system operates as an electrical storage to guarantee the demand requirements, as the batteries do actually in this and other systems. In this scenario, the external signals are not coming from the market, instead, they are generated by the unbalance between demand and renewable energy generated. This case is interesting in the context of small micro grids, as islands systems, where a storage system is often necessary to get a relevant share of renewables. Here, there are no explicit revenues as the system operates as a grid service, hence the economic evaluation has to be done from an investment point of view. However, modelling will be useful to optimize the sizing of the system components in order to minimize investment cost and maximize revenues.

4.2. Simulation environment

The simulation environment used in this project is TRNSYS 18 [19]. TRNSYS is a complete and extensible simulation environment for the transient simulation of systems, including multi-zone buildings. It is used by engineers and researchers around the world to model new energy

concepts, from simple domestic hot water systems to the design and simulation of buildings and their equipment, including control strategies, occupant behaviour, alternative energy systems (wind, solar, photovoltaic, hydrogen systems), etc.
One of the key factors in TRNSYS' success over the last 40 years is its open, modular structure. The source code of the kernel as well as the component models is delivered to the end users. This simplifies extending existing models to make them fit the user's specific needs.
TRNSYS applications include:

- Solar energy systems (solar thermal and PV)
- Low energy buildings and HVAC systems with advanced design features (natural ventilation, slab heating/cooling, double façade, etc.)
- Renewable energy systems
- Cogeneration, fuel cells
- Anything that requires dynamic simulation

To allow an evaluation of refrigerant properties in the model, we used CoolProp [20]. CoolProp is a C++ library that implements:

- Pure and pseudo-pure fluid equations of state and transport properties for 122 components
- Mixture properties using high-accuracy Helmholtz energy formulations
- Correlations of properties of incompressible fluids and brines
- Computational efficient tabular interpolation
- Highest accuracy psychrometric routines
- User-friendly interface around the full capabilities of NIST REFPROP
- Cubic equations of state

4.3. Component model description

4.3.1. Standard and commercial components

A screenshot of the model is shown in the next figure

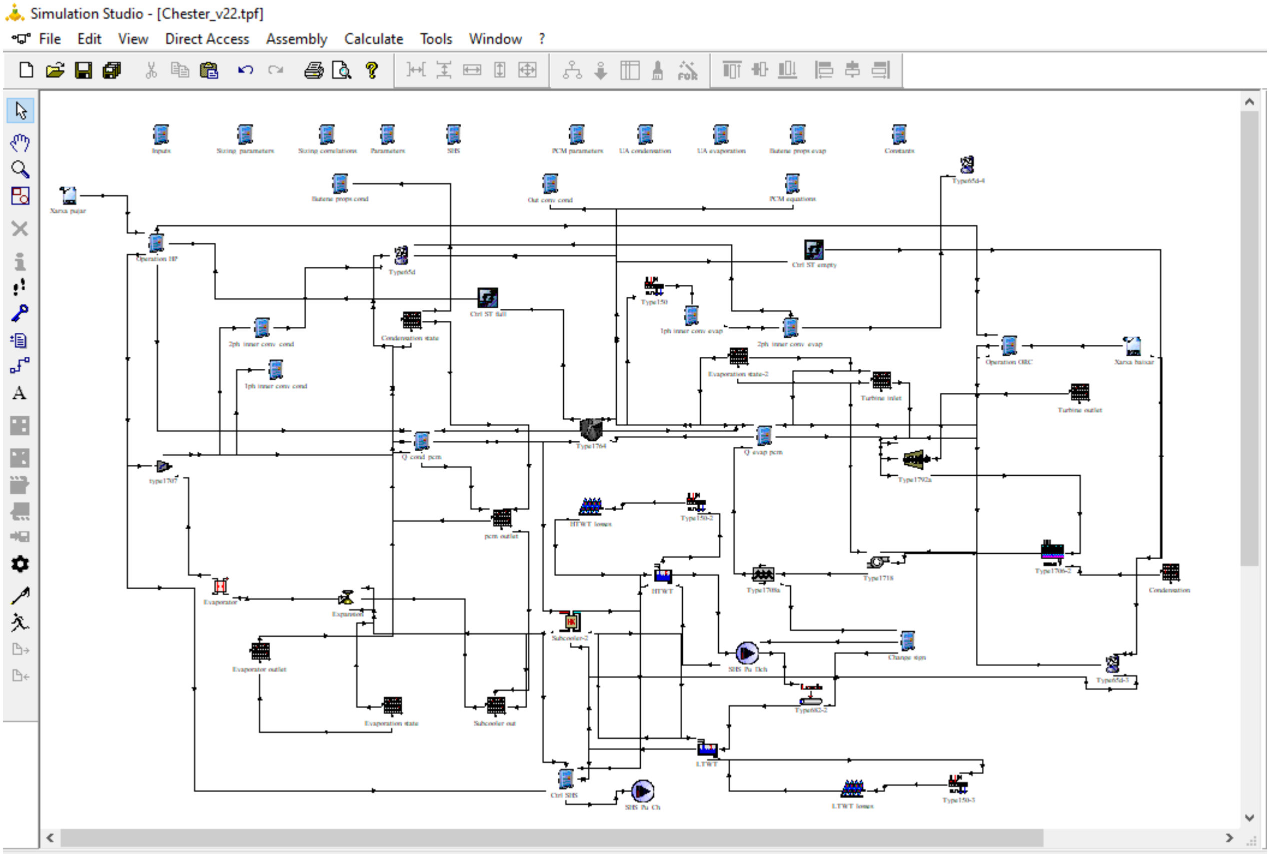

Figure 7: Screenshot of the CHEST model in the TRNSYS simulation environment

The model is structured in components, which are the icons in the model screenshot, representing pumps, compressor, etc. These components contain the equations involved in the calculation of each element, and the results from each of them (called outputs) are passed as inputs to other elements for their own calculations. After several iterations, the system converges and the simulation goes ahead with the next timestep, storing the desired outputs in files which can be processed at the end of the simulation.

In this model, components from three different sources have been used:

- Components from the TRNSYS standard libraries
- Components from the TESS commercial libraries
- Components developed specifically for the project

Many of the components developed in the project are modifications from the TESS Cogeneration libraries. The next table lists the components of the model:

Table 2: List of TRNSYS components in the model

Name	Component number	Description
Constants	TRNSYS equation block	A set of constant values used in the simulation like pi number, water density…
Inputs	TRNSYS equation block	A set of parameters used to define the current system: HP power, ORC power…

Sizing	TRNSYS equation block	A set of parameters used to size the current system, together with the inputs: PCM per HX length, heat transfer coefficient...
Sizing correlations	TRNSYS equation block	A set of parameters used to calculate the current system sizing: PCM HX length, number of pipes...
Parameters	TRNSYS equation block	A set of parameters of the simulation: HP superheating, subcooling,...
SHS	TRNSYS equation block	A set of parameters used to size the sensible heat storage: volumes, pump flows...
PCM parameters	TRNSYS equation block	A set of parameters in the PCM storage: melting temperature, conductivity...
UA condensation	TRNSYS equation block	A set of equations to calculate the UA of the condensation in the PCM storage
UA evaporation	TRNSYS equation block	A set of equations to calculate the UA of the evaporation in the PCM storage
Butene prop evap	TRNSYS equation block	A set of correlations to calculate some refrigerant properties at the PCM evaporator temperature
Butene prop cond	TRNSYS equation block	A set of correlations to calculate some refrigerant properties at the PCM condenser temperature
Out conv	TRNSYS equation block	A set of equations to calculate the convection coefficient within the PCM storage
PCM equations	TRNSYS equation block	A set of equations to calculate some PCM storage parameters: PCM volume, PCM mass...
Xarxa pujar	Type 9: data reader	An external file reader with market signals
Operation HP	TRNSYS equation block	A set of equations to set the operation state of the HP
Ctrl ST full	Type 2: Differential controller	Checks if the PCM storage is completely charged
Ctrl ST empty	Type 2: Differential controller	Checks if the PCM storage is completely discharged
1ph inner conv evap	TRNSYS equation block	A set of equations to calculate the evaporator inner convection coefficient for one phase flow
2ph inner conv evap	TRNSYS equation block	A set of equations to calculate the evaporator inner convection coefficient for two phase flow
1ph inner conv cond	TRNSYS equation block	A set of equations to calculate the condenser inner convection coefficient for one phase flow
2ph inner conv cond	TRNSYS equation block	A set of equations to calculate the condenser inner convection coefficient for two phase flow
Condensation state	Type 1234: CoolProp call	Used to calculate the thermodynamic properties of refrigerant at the PCM condensation state

Evaporation state	Type 1234: CoolProp call	Used to calculate the thermodynamic properties of refrigerant at the PCM evaporation state
Xarxa baixar	Type 9: data reader	An external file reader with market signals
Operation ORC	TRNSYS equation block	A set of equations to set the operation state of the ORC
Turbine inlet	Type 1234: CoolProp call	Used to calculate the thermodynamic properties of refrigerant at the turbine inlet
Turbine outlet	Type 1234: CoolProp call	Used to calculate the thermodynamic properties of refrigerant at the turbine outlet
Compressor	Type 1707: Isentropic compressor	Models the compressor
Q cond pcm	TRNSYS equation block	A set of equations to calculate the PCM condenser heat transfer
Q evap pcm	TRNSYS equation block	A set of equations to calculate the PCM evaporator heat transfer
PCM	Type 1764: Capacitance PCM storage	Models the PCM storage
ORC	Type 1792: Isentropic turbine	Models the ORC turbine
PCM outlet	Type 1234: CoolProp call	Used to calculate the thermodynamic properties of refrigerant at the PCM condenser outlet
Condensation	Type 1234: CoolProp call	Used to calculate the thermodynamic properties of refrigerant at the condenser outlet
HTWT losses	Type 1226: Tank gas heater	Used to compensate the thermal losses of the HTWT
Losses 1	Type 150: delayed inputs	Used to calculate the thermal losses of the HTWT
LTWT losses	Type 1226: Tank gas heater	Used to compensate the thermal losses of the LTWT
Losses 2	Type 150: delayed inputs	Used to calculate the thermal losses of the LTWT
HTWT	Type 39: Variable volume storage	Models the high temperature sensible storage
LTWT	Type 39: Variable volume storage	Models the low temperature sensible storage
Preheater	Type 1708: Condensate preheater	Models the ORC loop preheater
Pump	Type 1718: Condensate pump	Models the condensate pump
Condenser	Type 1706: Refrigerant condenser	Models the ORC loop condenser
Evaporator	Type 1703: Refrigerant evaporator	Models the HP loop evaporator
Expansion	Type 1704: expansion device	Models the isenthalpic expansion of the HP loop

Evaporator outlet	Type 1234: CoolProp call	Used to calculate the thermodynamic properties of refrigerant at the evaporator outlet
Evaporation state	Type 1234: CoolProp call	Used to calculate the thermodynamic properties of refrigerant at the evaporation state
Subcooler out	Type 1234: CoolProp call	Used to calculate the thermodynamic properties of refrigerant at outlet of the evaporator
Subcooler	Type 699: HX with cold side control	Models de HP loop subcooler
SHS Pu Ch	Type 110: Variable speed pump	Models de pump of the SHS when charging
SHS Pu Dch	Type 110: Variable speed pump	Models the pump of the SHS when discharging
Ctrl SHS	TRNSYS equation block	A set of equations to set the operation state of the SHS pump when charging
Ctrl DCh	TRNSYS equation block	A set of equations to set the operation state of the SHS pump when discharging

The TRNSYS and TESS libraries documentation explains in detail the characteristics and mathematical description of each of the standard and commercial models. The description of the types developed in the project is included in the next sections.

4.4. HP component models

4.4.1. Compressor model

The compressor model relies on an isentropic efficiency approach method to characterize the compressor performance. It was developed specifically for the model of the CHESTER project in such a way that the compressor control is linked to the control of the CHEST system. As explained in section 3.4, the CHEST system has to deal with an externally imposed electricity consumption, so the electricity consumption of the compressor has to be kept constant and equal to the amount bided by the CHEST operator for that time period. The compressor model, uses the evaporator outlet conditions and the required condensation temperature to calculate the amount of refrigerant that can be compressed with the current time electrical input.

The compressor model has the following parameters, inputs and outputs:

PARAMETERS

1	Motor power	[kW]	Motor maximum electric power
2	Evaporator temperature	[C]	Refrigerant evaporator temperature
3	Refrigerant number	[-]	CoolProp code for working refrigerant
4	Heat loss	[-]	Compressor thermal losses, relative to compressor work

INPUTS

1	Inlet flowrate	[kg/h]	Refrigerant flowrate at compressor suction
2	Electrical efficiency	[-]	Compressor motor electrical efficiency
3	Isentropic efficiency	[-]	Compressor isentropic efficiency
4	Superheating temperature	[C]	Superheating temperature at evaporator outlet
5	Control signal	[-]	ON/OFF signal for starting the compressor
6	Pressure loss	[kPa]	Pressure loss at compressor suction
7	Condenser temperature	[C]	Desired condensing pressure

OUTPUTS

1	Motor consumption	[kW]	Electrical consumption by the compressor
2	Compressor flowrate	[kg/h]	Compressor discharge flowrate
3	Specific volume	[m³/kg]	Refrigerant specific volume at compressor suction
4	Outlet enthalpy	[kJ/kg]	Refrigerant enthalpy at discharge
5	Outlet pressure	[kPa]	Refrigerant pressure at discharge
6	Thermal losses	[kW]	Compressor thermal losses
7	Outlet temperature	[C]	Refrigerant temperature at discharge

MATHEMATICAL DESCRIPTION

The model first uses the input of evaporator temperature, to call CoolProp with quality set to 1 to get the refrigerant properties at the evaporator: density, enthalpy, entropy and pressure. With the evaporator pressure and the superheating temperature, it calls CoolProp again to get the refrigerant conditions at the evaporator outlet, and with the resulting temperature and the pressure at the evaporator outlet minus the suction pressure drop (input 6), calls again CoolProp to get the properties of the refrigerant at the inlet of the compressor (in particular, the enthalpy).

Next, the model uses the condensing temperature (Input 7) and quality set to 0 to call CoolProp and get the condensing pressure. The compressor discharge pressure is assumed to be the same as the condensing pressure.

After this, the compressor calculates the enthalpy of the isentropic compression, calling again CoolProp with the pressure set to the discharge pressure and the entropy of the refrigerant at the inlet of the compression. With this, it calculates the discharge enthalpy as:

$$h_{dis} = h_{suc} + (h_{is} - h_{suc})/Isen\_eff$$

Where the subscripts *dis*, *suc* and *is* refer to the discharge, suction and isentropic compression states calculated previously from CoolProp, and Isen_eff stands for the compressor isentropic efficiency. Then, the energy delivered by the compressor to the refrigerant is calculated according to:

$$\dot{W}_{acc} = W_{in} \cdot Elec\_eff \cdot (1 - r_{loss})$$

Where r_{loss} includes the thermal losses from the compressor, Elec_eff is the motor electrical efficiency (Input 3) and W_{in} is the electrical energy absorbed by the compressor (Input 1).. Finally, the compressor flow rate is calculated according to

$$m_{suc} = W_{acc}/(h_{dis} - h_{suc})$$

Where h_{dis} and h_{suc}. Refer to the enthalpy at the inlet and outlet of the compressor, respectively.

The condensing temperature is calculated externally to the compressor model based on the heat transfer coefficient at the condenser (see section 4.7.1 for a detailed description of how this is calculated). Based on the heat transfer coefficient and the required electricity consumption, two equations are taken into account. First, the heat released at the condenser has to fulfill:

$$Q_{condenser} = h \cdot A \cdot (T_{condensing} - T_{PCM})$$

Where h stands for the heat transfer coefficient at the condenser, A is the area of the condenser and $T_{condensing}$ is the current condensing temperature and T_{PCM} is the temperature at the PCM storage. The second equation used is

$$Q_{condenser} = \dot{m} \cdot \Delta h$$

Where m (dotted) refers to the mass flow at the condenser (assumed the same as the compressor flow rate) and the delta h refers here to the enthalpy difference through the condenser. Equaling these two equations, we get a relationship between condensing temperature and the flow rate. The flow rate however is an output from the compressor model, so TRNSYS iterates until reaching a solution for both the condensing temperature and the flowrate.

4.4.2. Expansion device model

This model calculates the performance of a refrigerant pressure-reducing valve. The refrigerant at the inlet of the valve adiabatically expands to the specified outlet pressure. If the desired outlet pressure is above the inlet refrigerant pressure the refrigerant passes through the device without a change in state.

The expansion device model has the following parameters, inputs and outputs:

PARAMETERS

1	Refrigerant code	[-]	CoolProp code for the refrigerant in use

INPUTS

1	Inlet refrigerant temperature	[C]	Temperature of refrigerant at the inlet of the valve
2	Inlet refrigerant flowrate	[kg/h]	Mass flow of refrigerant at the inlet of the valve
3	Inlet refrigerant enthalpy	[kJ/kg]	Enthalpy of refrigerant at the inlet of the valve
4	Inlet refrigerant pressure	[kPa]	Pressure of refrigerant at the inlet of the valve
5	Outlet pressure set point	[kPa]	Desired pressure at the outlet of the device

OUTPUTS

1	Outlet refrigerant temperature	[C]	Temperature of refrigerant at the outlet of the valve

2	Outlet refrigerant flowrate	[kg/h]	Mass flow of refrigerant at the outlet of the valve
3	Outlet refrigerant enthalpy	[kJ/kg]	Enthalpy of refrigerant at the outlet of the valve
4	Outlet refrigerant pressure	[kPa]	Pressure of refrigerant at the outlet of the valve

MATHEMATICAL DESCRIPTION

The model calculations start by comparing the inlet pressure with the pressure setpoint at the outlet; if the second is greater, then the fluid goes out of the valve unchanged. Otherwise, the model assumes an isenthalpic expansion of the system, and calls the CoolProp database to calculate the refrigerant properties with a pressure equal to the user setpoint and the inlet enthalpy to determine the outlet properties of the refrigerant.

4.4.3. HP loop evaporator model

This model simulates a counter-flow evaporator for refrigeration applications. The model attempts to meet the specified refrigerant outlet condition but may be limited by the entering hot-side temperatures and flow rate. The model relies on the pinch-point temperature difference approach to check for unaffordable heat exchange conditions. The pinch-point temperature difference is defined to be the minimum temperature difference between the hot-source fluid and the refrigerant that allows for heat transfer between the fluids. The pinch-point is checked at the outlet of the refrigerant flow (as well, inlet of the hot source flow), the outlet of the hot source flow (the refrigerant inlet), at the refrigerant saturated liquid point, and at the refrigerant saturated vapor point. If the temperature difference at these points is less than the pinch-point temperature difference, the heat transfer is re-calculated such that the pinch-point problem is not encountered.

The HP loop evaporator model has the following parameters, inputs and outputs:

PARAMETERS

1	Pinch point temperature	[K]	Minimum temperature difference between both flows along the HX
2	Source C_p	[kJ/(kg·K)]	Thermal capacity of the source fluid
3	Refrigerant code	[-]	CoolProp code for the refrigerant in use
4	Refrigerant critical density	[kg/m^3]	Refrigerant critical density
5	Refrigerant side pressure drop	[kPa]	Pressure drop in the HX refrigerant side

INPUTS

1	Source temperature	[°C]	Inlet temperature of the hot fluid
2	Source flow rate	[kg/h]	Inlet mass flow of the hot fluid
3	Inlet refrigerant temperature	[C]	Temperature of refrigerant at the inlet of the evaporator
4	Inlet refrigerant flowrate	[kg/h]	Mass flow of refrigerant at the inlet of the evaporator
5	Inlet refrigerant enthalpy	[kJ/kg]	Enthalpy of refrigerant at the inlet of the evaporator

6	Inlet refrigerant pressure	[kPa]	Pressure of refrigerant at the inlet of the evaporator
7	Refrigerant outlet setpoint	[°C]	Desired outlet temperature of the refrigerant

OUTPUTS

1	Outlet source temperature	[°C]	Outlet temperature of the hot fluid
2	Outlet source flow rate	[kg/h]	Outlet mass flow of the hot fluid
3	Outlet refrigerant temperature	[°C]	Temperature of refrigerant at the outlet of the valve
4	Outlet refrigerant flowrate	[kg/h]	Mass flow of refrigerant at the outlet of the evaporator
5	Outlet refrigerant enthalpy	[kJ/kg]	Enthalpy of refrigerant at the outlet of the evaporator
6	Outlet refrigerant pressure	[kPa]	Pressure of refrigerant at the outlet of the evaporator
7	Heat transfer rate	[kJ/h]	Rate of energy transfer from the hot fluid to the refrigerant

MATHEMATICAL DESCRIPTION

The model first checks 1) if the inlet flow rate of any of both sides of the heat exchanger is 0 and 2) if the inlet enthalpy is bigger than the desired enthalpy; if any of this conditions is true, then nothing happens inside the model and the outputs are set equal to the inputs.

Then, the model makes several calls to the CoolProp routine to determine the following states:

- Saturation temperature of the entering refrigerant
- Enthalpy of the saturated liquid refrigerant
- Enthalpy of the saturated vapour refrigerant
- Enthalpy of the desired outlet state

With this information the model calculates:

- The energy required to heat the refrigerant to the saturation liquid state
- The energy required to heat the refrigerant to the saturation vapour state
- The energy required to heat the refrigerant to the required superheated state

After this, the model determines if the inlet state and the outlet desired state for the refrigerant is either subcooled, saturated or superheated and the outlet state of both fluids in case that the system would be able to meet the required conditions. Finally, based on the inlet and desired outlet state, the pinch point limitation is evaluated at different points of the heat exchanger. If the pinch point is violated, the temperatures are recalculated according to the pinch point and the energy transfer is determined.

4.5. PCM storage model

The PCM storage model is modelled as a thermal mass with variable, temperature dependent, capacitance. Different heat fluxes can be released in this capacitance, and the model determines the temperature of the mass by solving a simple first order differential equation. As explained in section 4.7.1, the lumped capacitance approach is not valid for solids where the Biot number is bigger than 1, since in that case, a temperature gradient develops in the interior of the solid that has a very relevant effect on the effective heat transfer. There is however the possibility of using this approximation in the case that the heat transfer coefficient is corrected considering the solid body geometry, which is the approach we have followed to simplify the calculation of the PCM storage and to reduce computation time.

The PCM storage model has the following parameters, inputs and outputs:

PARAMETERS

1	Energy flows	[-]	Number of energy flows entering or exiting the storage without considering environmental thermal losses
2	Area	[m^2]	External surface area of the storage
3	Initial temperature	[°C]	Temperature of the storage at the beginning of the simulation
4	Mass	[kg]	Mass of PCM within the storage
5	Solid C_p	[kJ/kg·K]	Thermal capacity of the PCM in solid state
6	Phase change enthalpy	[kJ/kg]	Latent heat of fusion of the PCM
7	Liquid C_p	[kJ/kg·K]	Thermal capacity of the PCM in liquid state
8	Melting temperature	[°C]	Melting temperature of the PCM
9	Temperature increase in melting	[°C]	The model allows an increase of temperature while melting as a simplification (use 1°C)

INPUTS

1	Environmental temperature	[°C]	Temperature surrounding the PCM
2	U value	[kJ/h·m^2·K]	The heat transfer coefficient of the storage with the environment
3	Heat gain	[kJ/h]	The rate at which heat is added or extracted from the storage. There are as many as the value of Parameter 1. Positive values are energy inputs (condenser) and negatives are energy outputs (evaporator) from the storage

OUTPUTS

1	Storage temperature	[°C]	Average storage temperature

2	Heat loss	[kJ/h]	Heat loss to the environment
3	Energy gain	[kJ/h]	Sum of the energy flows into the storage
4	Energy storage rate	[kJ/h]	The rate at which the storage is storing energy

MATHEMATICAL DESCRIPTION

The model uses a thermal capacitance approach to model the PCM storage. This thermal capacitance is a function of the storage temperature according to the following expression

$$Cp(T) = \begin{cases} Cp^{solid} & T < T_{melt} \\ Cp^{melting} & T_{melt} < T < T_{melt} + dT_{melt} \\ Cp^{liquid} & T > T_{melt} + dT_{melt} \end{cases}$$

Where C_p^{solid} and C_p^{liquid} are the thermal capacities of the PCM in liquid or solid state (parameters 5 and 7) multiplied by the PCM storage mass and $C_p^{melting}$ is defined like:

$$C_p^{melting} = \frac{Mass_{\ PCM} \Delta H_{fusion}}{dT_{melt}}$$

Where ΔH_{fusion} is the latent heat of fusion of the PCM (parameter 6), $Mass_{PCM}$ is the mass of PCM in the storage (parameter 4) and dT_{melt} is the temperature increase while melting (parameter 9).

To keep the model simple, a slight temperature increase is allowed to the system while the transition from solid to liquid, called dT_{melt} in the previous expression. We recommend to set this value to 1 °C in order to keep the approximation effect in the heat transfer small.

At each time step, the model determines the phase state of the storage material based on the temperature at the end of the previous time step: solid, if under the melting temperature; fluid if the temperature is higher than melting temperature+ parameter nine; and melting otherwise.

After that, the model calculates the energy required by the storage to reach the temperature of the boundaries of phase change, T_{melt} and T_{melt} +dT_{melt}, and calculates the overall heat flux within the storage, summing up all the user defined heat flows. A positive energy flux is an energy gain of the system (storage charging) and a negative energy flux is an energy loss of the system (storage discharging).

By comparing the sum of all the energy input to the storage with the energies required to reach phase change, the model determines the phase state of the storage at the end of the current time step: solid, fluid or melting state. If a transition takes place, the storage temperature is updated to the boundary value from the state at the beginning of the time step to the state at the end of the time step (either T_{melt} or T_{melt}+dT_{melt}), and the energy flow is recalculated as

$$\dot{Q} = \begin{cases} \sum \dot{Q}_i \ if\ j = k \\ \sum \dot{Q}_i - \dot{Q}_{boundary} \ \ if\ j \neq k \end{cases}$$

Where j and k refer to the initial and final phase state and $Q_{boundary}$ refers to the energy required to reach the phase change.

To determine the final temperature of the storage, the model then solves the first order heat transfer differential equation

$$\sum \dot{Q}_i = C_p \frac{dT}{dt}$$

Where C_p is the capacitance of the PCM at the final state, dt is the simulation time step, dT the temperature increase in the current time step and Q_i is sum of the energy flows:

$$\sum Q_i = \dot{Q} + \dot{Q}_{losses} = \dot{Q} + U_{value} \cdot A_{external} \cdot (T - T_{amb})$$

Where Q_{losses} is the thermal losses from the storage to the ambient, U_{value} is the heat transfer coefficient of the storage (input 2) and $A_{external}$ is the area of the storage in contact with the ambient and T_{amb} is the ambient temperature (input 1). Substituting in the previous equation:

$$\frac{\dot{Q}}{C} + \frac{U_{value} \cdot A_{external} \cdot (T - T_{amb})}{C} = \frac{dT}{dt}$$

Where Q dotted is the sum of energy flows in kJ/h into or out of the PCM storage. Every energy flow includes the appropriate driving temperature difference (T-Ti) for the current time step, e.g. between the refrigerant and the PCM. (T-Tamb) is driving temperature difference between the PCM and the environment of the storage for the current time step. And dT is the temperature difference between the time steps, dT=Tnew-Told. U is the thermal losses coefficient (Input 2) and A is the external surface area (parameter 2). This equation is solved by the TRNSYS differential equation solver to determine the temperature of the storage at the end of the timestep. With this, the thermal losses can be calculated as:

$$\dot{Q}_{losses} = U_{value} \cdot A_{external} \cdot (T_{final} - T_{amb})$$

Where T_{final} is the temperature of the storage at the end of the time step and T_{amb} is the surrounding temperature.

Then the stored energy is

$$Q_{stored} = C \cdot (T_{final} - T_i)/timestep$$

Where T_i is the initial temperature of the storage in the current time step if there has been no phase change, or the boundary temperature of the phase change if there was a phase change in the current time step.

4.6. ORC loop component models

4.6.1. ORC expander model

The ORC expander is modelled by an isentropic efficiency approach and uses CoolProp to determine the state of the working fluid at different points in the expander. It is possible to define injections and extractions in case a more elaborated layout of the system is necessary.

The ORC expander model has the following parameters, inputs and outputs:

PARAMETERS

1	Rated Expander power	[kJ/h]	Electrical power of the turbine
2	Number of injections	[-]	Number of injections into the expander
3	Number of extractions	[-]	Number of extractions from the expander
4	Refrigerant flag	[-]	CoolProp code for the refrigerant in use

INPUTS

1	Inlet refrigerant temperature	[°C]	Temperature of refrigerant at the inlet of the expander
2	Inlet refrigerant flowrate	[kg/h]	Mass flow of refrigerant at the inlet of the valve
3	Inlet refrigerant enthalpy	[kJ/kg]	Enthalpy of refrigerant at the inlet of the valve
4	Inlet refrigerant pressure	[kPa]	Pressure of refrigerant at the inlet of the valve
5	Exhaust pressure	[kPa]	Refrigerant pressure at the outlet of the turbine
6	Control signal	[-]	Input signal (0/1) to set if the expander is operating
7	Isentropic efficiency	[-]	Turbine isentropic efficiency

OUTPUTS

1	Outlet refrigerant temperature	[°C]	Temperature of refrigerant at the outlet of the valve
2	Outlet refrigerant flowrate	[kg/h]	Mass flow of refrigerant at the outlet of the valve
3	Outlet refrigerant enthalpy	[kJ/kg]	Enthalpy of refrigerant at the outlet of the valve
4	Outlet refrigerant pressure	[kPa]	Pressure of refrigerant at the outlet of the valve
5	Power produced	[kJ/h]	Power produced by the turbine
6	Isentropic efficiency	[-]	Expander isentropic efficiency
7	PLR	[-]	Expander part load ratio

MATHEMATICAL DESCRIPTION

The expander model has been developed with the aim of coupling it with the rest of the CHEST TRNSYS model. To fit within the system control scheme, the turbine operates at theoretical maximum power output given the mass flow rate at the inlet, the inlet refrigerant conditions, the turbine back pressure and the isentropic efficiency.

To calculate the power produced at the current conditions, the model uses CoolProp to calculate the refrigerant state at the outlet, calling it with the pressure at the condenser and the refrigerant outlet temperature, calculated as:

$$h_{out} = h_{in} - \eta_{is}(h_{in} - h_{is})$$

Where η_{is} is the turbine isentropic efficiency and h_{is} is the enthalpy at the inlet entropy conditions and the turbine backpressure. With this, the work is simply calculated as

$$\dot{W} = \dot{m}_{in} \cdot (h_{in} - h_{out})$$

4.6.1. ORC condenser model

This model represents a condenser for refrigeration applications where the condensing pressure is imposed. The model calculates the resulting heat transfer and outlet refrigerant conditions based on the desired degrees of subcooling at the outlet of the condenser.

The ORC condenser model has the following parameters, inputs and outputs:

PARAMETERS

1	Refrigerant flag	[-]	CoolProp code for the refrigerant in use

INPUTS

1	Inlet refrigerant temperature	[°C]	Temperature of refrigerant at the inlet
2	Inlet refrigerant flowrate	[kg/h]	Mass flow of refrigerant at the inlet
3	Inlet refrigerant enthalpy	[kJ/kg]	Enthalpy of refrigerant at the inlet
4	Inlet refrigerant pressure	[kPa]	Pressure of refrigerant at the inlet
5	Condensing pressure	[kPa]	Refrigerant condensing pressure
6	Subcooling	[K]	Degrees of subcooling at the outlet of the condenser

OUTPUTS

1	Condensate refrigerant temperature	[°C]	Temperature of refrigerant at the outlet
2	Condensate refrigerant flowrate	[kg/h]	Mass flow of refrigerant at the outlet
3	Condensate refrigerant enthalpy	[kJ/kg]	Enthalpy of refrigerant at the outlet
4	Condensate refrigerant pressure	[kPa]	Pressure of refrigerant at the outlet
5	Heat transfer	[kJ/h]	Condenser heat transfer rate

MATHEMATICAL DESCRIPTION

The model uses several calls to CoolProp to determine the refrigerant conditions during the condensing process. Initially, the inlet values are called and checked for problems, and the condensing state is determined by calling CoolProp with quality set to zero and the lowest value of pressure from the inlet pressure and the condensing pressure.

The outlet state is calculated from there by calling CoolProp with the condensing temperature minus the degrees of subcooling and the minimum of the inlet and the condensing pressure. With this, the outlet conditions of the condensate are determined and the heat transfer rate is calculated as

$$\dot{Q}_{cond} = \dot{m} \cdot (h_{in} - h_{out})$$

It is worth to note that the component does not make any calculation on the secondary fluid, that has to be managed externally to ensure energy balance.

4.6.2. ORC preheater model

This model simulates a condensate preheater for refrigeration applications. The model attempts to meet the specified refrigerant outlet condition but may be limited by the entering hot-side temperatures and flow rate. The model relies on a fixed pinch-point temperature difference to describe the heat transfer behaviour. The pinch-point temperature difference is defined as the minimum temperature difference between the two streams that allows for heat transfer between the fluids. The pinch-point is checked at the outlet of the condensate flow (as well, inlet of the hot source flow), the outlet of the hot source flow (the condensate inlet), and at the condensate saturated liquid point. If the temperature difference at these points is less than the pinch-point temperature difference, the heat transfer is re-calculated such that the pinch-point temperature difference is satisfied.

The ORC preheater model has the following parameters, inputs and outputs:

PARAMETERS

1	Pinch point temperature	[K]	Minimum temperature difference between both flows along the HX
2	Source C_p	[kJ/(kg·K)]	Thermal capacity of the source fluid
3	Condensate C_p	[kJ/(kg·K)]	Thermal capacity of the condensate
4	Subcooling temperature	[°C]	Temperature difference between condensate outlet conditions and saturation conditions
5	HX configuration	[-]	Not used
6	Refrigerant code	[-]	CoolProp code for the refrigerant in use

INPUTS

1	Source temperature	[°C]	Inlet temperature of the hot fluid
2	Source flow rate	[kg/h]	Inlet mass flow of the hot fluid
3	Inlet refrigerant temperature	[°C]	Temperature of refrigerant at the inlet of the HX
4	Inlet refrigerant flowrate	[kg/h]	Mass flow of refrigerant at the inlet of the valve
5	Inlet refrigerant enthalpy	[kJ/kg]	Enthalpy of refrigerant at the inlet of the valve

6	Inlet refrigerant pressure	[kPa]	Pressure of refrigerant at the inlet of the valve
7	Refrigerant outlet setpoint	[°C]	Desired outlet temperature of the refrigerant

OUTPUTS

1	Outlet source temperature	[°C]	Outlet temperature of the hot fluid
2	Outlet source flow rate	[kg/h]	Outlet mass flow of the hot fluid
3	Condensate refrigerant temperature	[°C]	Temperature of refrigerant at the outlet
4	Condensate refrigerant flowrate	[kg/h]	Mass flow of refrigerant at the outlet
5	Condensate refrigerant enthalpy	[kJ/kg]	Enthalpy of refrigerant at the outlet
6	Condensate refrigerant pressure	[kPa]	Pressure of refrigerant at the outlet
7	Condensate refrigerant temperature	[°C]	Temperature of refrigerant at the outlet

MATHEMATICAL DESCRIPTION

The model first checks 1) if the inlet flow rate of any of both sides of the heat exchanger is 0 and 2) If the inlet enthalpy is bigger than the desired enthalpy; if any of this conditions is true, then nothing happens inside the model and outputs are set equal to the inputs.

Then, the model makes several calls to the CoolProp routine to determine the following states:

- Saturation temperature of the entering refrigerant
- Enthalpy of the saturated liquid refrigerant
- Enthalpy of the desired outlet state

With this information the model calculates:

- The energy required to heat the refrigerant to the saturation liquid state
- The energy required to heat the refrigerant to the required outlet state

After this, the model determines if the inlet state and the outlet desired state for the refrigerant is either subcooled, saturated or superheated and the outlet state of both fluids in case that the system would be able to meet the required conditions. Finally, based on the inlet and desired outlet state, the pinch point limitation is evaluated at different points of the heat exchanger. If the pinch point is violated, the temperatures are recalculated according to the pinch point and the energy transfer is determined.

4.6.3. Pump model

This component models a pump. Based on the inlet conditions and the desired outlet pressure the model calculates the theoretical power needed.

The condensate pump model has the following parameters, inputs and outputs:

PARAMETERS

1	Pump efficiency	[-]	The pump overall efficiency
2	Motor efficiency	[-]	The pump motor efficiency (must be greater than the pump overall efficiency)
3	Refrigerant code	[-]	CoolProp code for the refrigerant in use

INPUTS

1	Inlet refrigerant temperature	[°C]	Temperature of refrigerant at the inlet of the condensate pump
2	Inlet refrigerant flowrate	[kg/h]	Mass flow of refrigerant at the inlet
3	Inlet refrigerant enthalpy	[kJ/kg]	Enthalpy of refrigerant at the inlet
4	Inlet refrigerant pressure	[kPa]	Pressure of refrigerant at the inlet
5	Inlet refrigerant enthalpy	[kJ/kg]	Enthalpy of refrigerant at the inlet
6	Setpoint outlet pressure	[kPa]	Required pressure of refrigerant at the outlet
7	Control signal	[-]	Input signal (between 0 and 1) to set if the pump is operating

OUTPUTS

1	refrigerant flowrate	[kg/h]	Mass flow of refrigerant at the outlet
2	refrigerant enthalpy	[kJ/kg]	Enthalpy of refrigerant at the outlet
3	refrigerant pressure	[kPa]	Pressure of refrigerant at the outlet
4	refrigerant temperature	[°C]	Temperature of refrigerant at the outlet
5	Ideal pump power	[kJ/h]	Ideal pump power consumption
6	Theoretical pump power	[kJ/h]	Pump power consumption divided by the pump efficiency
7	Environmental losses	[kJ/h]	The energy lost to the environment by the pump motor

MATHEMATICAL DESCRIPTION

The model first determines the pumping efficiency with the parameters 1 and 2 as

$$\eta_{pumping} = \frac{\eta_{pump}}{\eta_{motor}}$$

Then the work required to increase the condensate pressure is calculated by calling CoolProp to get the specific volume of the condensate inlet (v_{inlet}) and the following equation:

$$\dot{W} = \dot{m}_{condensate} \cdot v_{inlet} \cdot (p_{out} - p_{in})$$

Where p_{out} and p_{in} are the outlet and inlet pressures. Then the pump shaft power and the pump power consumption are calculated as

$$P_{shaft} = \frac{\dot{W}}{\eta_{pumping}}$$

$$P_{pump} = \frac{P_{shaft}}{\eta_{motor}}$$

Part of the energy consumption of the pump is transferred to the condensate as thermal energy, and this is accounted for by

$$\dot{Q}_{condensate} = P_{shaft} \cdot (1 - \eta_{pumping})$$

The rest of the energy lost by the motor is assumed to be released to the ambient as heat

$$\dot{q}_{ambient} = P_{pump} - \dot{q}_{condensate}$$

The outlet enthalpy of the condensate is calculated with the next equation

$$h_{out} = h_{in} + \frac{\dot{q}_{condensate}}{\dot{m}_{cond}}$$

Where m_{cond} is the inlet flow rate. Finally, the outlet refrigerant properties are calculated by calling CoolProp with the calculated outlet enthalpy and the desired outlet pressure.

4.7. System model description

The modelling work of the CHEST system is an integration effort of several technologies that have different dynamics, and those have to be matched in order to realistically represent the performance of the whole system. The three main interacting elements of the system are the heat pump, the ORC turbine and the PCM storage, and they have to operate according to the external electrical network status. The next figure, taken from [21] shows a schematic of the modelled system.

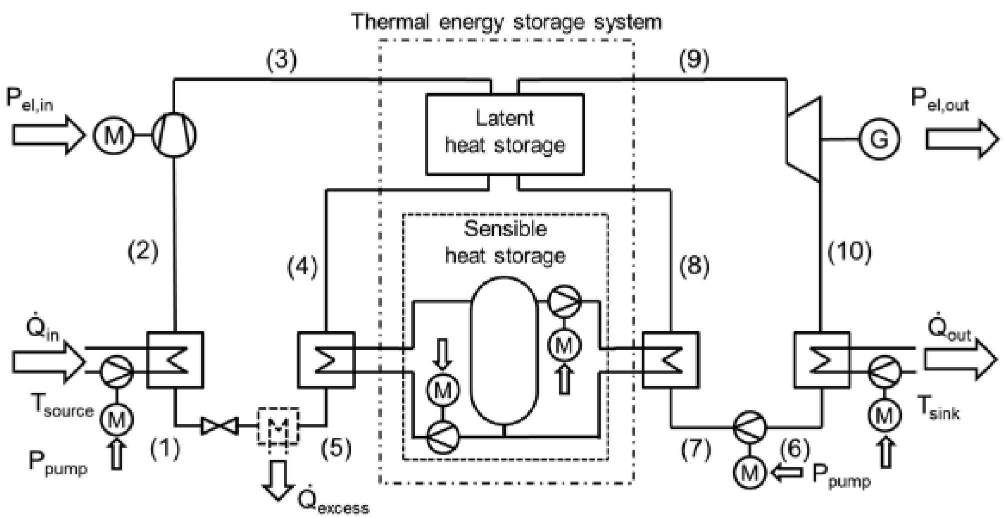

Figure 8: Schematic layout of the CHEST system modelled [21]

The system has two coupled refrigerant cycles, one with a heat pump and the other with an ORC turbine. The electricity is stored in the form of heat generated by the heat pump and stored in the latent heat storage to be used as a heat source by the ORC turbine who generates electricity while discharging the stored electricity. As a starting point for modelling the system, we considered butene as heat transfer medium and a lithium nitrate salt as a PCM material, since this has been previously identified as good candidates for the CHEST system in low temperature applications [21]. Other models of the system published, like [22] or [23], deal with CHEST concepts operating at much higher storage temperature. However, with the aim of allowing for optimization of these materials in T4.4 they have been used for developing the model in T4.2. Other fluids and PCMs will be investigated further in T4.4 by means of the model to compare the performance of the system and allow a better system performance under the particular circumstances of each case study.

When looking at the characteristics of the system, the main difference with standard heat pump or ORC applications is that the condenser, in the case of the heat pump cycle and the evaporator, for the ORC turbine cycle is inside the PCM material. This has implications in the concept design, since being the PCM often a solid material while operating, there is no means to control the heat released and absorbed in the PCM, as opposed to the most common condenser/evaporation devices that use a liquid or a gas as heat transfer medium (and hence they are usually pumped to modulate the heat transfer to the required process demand).

Due to this, the core of the modelling effort was to characterize the heat transfer at the PCM heat exchangers, since it is the less controllable dynamic of the system. The next section describes the heat transfer calculation equations involved in the model, which play a central role in the model of the CHEST system.

4.7.1. Heat transfer calculation in the storage HX

The calculation of heat transfer inside the PCM storage HX pipes in TRNSYS model is explained in this section. The model assumes a cylindrical geometry of the storage and the heat exchanger pipes are embedded there, surrounded by the PCM. The geometry of the heat exchanger is shown in Figure 9 [24]:

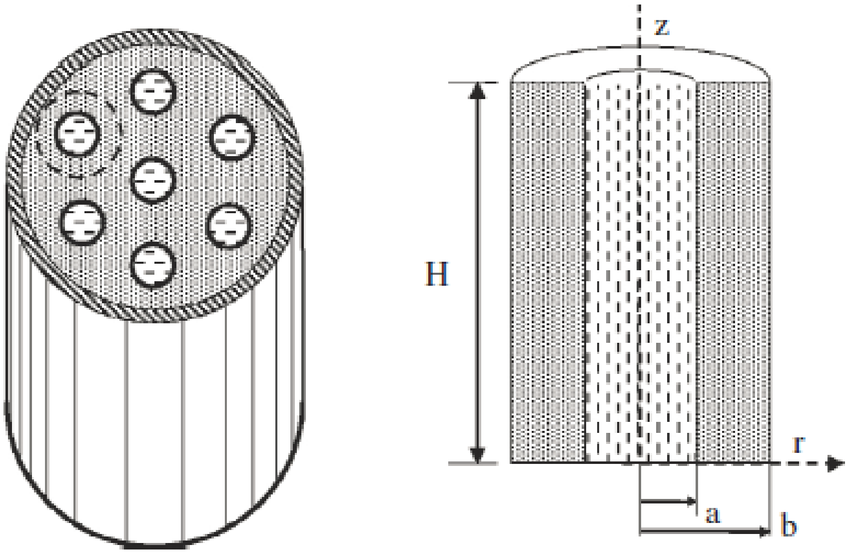

Figure 9: Solid thermal storage material with heat exchanger tubes [24]

The heat transfer inside one tube is obtained with the following equation [25]:

$$\dot{q} = \bar{h} \cdot A \cdot (DTLM)$$

Where h is the average heat transfer coefficient, A is the area of the pipe and DTLM is the mean logarithmic temperature difference. The difficulty of the problem stays on determining the heat transfer coefficient, in particular during two-phase flow, as it happens in the case of the CHEST system during condensation and evaporation of refrigerant inside the PCM storage.

In the process of determining the heat transfer, five terms are taken into account:

1. The convective heat transfer of the refrigerant inside the pipes
2. The thermal resistance of the pipe to conduction
3. The convection of the PCM material (when melting)
4. The conductivity of the PCM material
5. The heat enhancement due to finned tubes

The first is calculated with different equations in the condenser and the evaporator, but the others are not dependent of the phase change process of the refrigerant.

To calculate the heat transfer in the pipe, first we account for the convective heat transfer inside the tubes and the pipe thermal resistance. This can be calculated like [26]:

$$R_{tot} = \frac{1}{h_i \cdot 2\pi r_i \cdot L} + \frac{\ln\left({}^{r_o}/_{r_i}\right)}{2\pi \cdot \lambda \cdot L}$$

Where the thermal resistance is normalized to the pipe length, L, (thus it has units of K/(m·W)) and h_i is the inner convection coefficient, r_i and r_o are the inner and outer radius of the pipe and λ is the thermal conductivity of the pipe material.

The heat transfer coefficients h_i for evaporation and condensation are calculated by experimental correlations generated by fitting experimental data to analytical expressions. Several correlations for condensation [27] and evaporation [28] have been published in the scientific literature so far; they often present notable mean deviations from the experimental data, between 5 % and 15 %, due to the complex nature of these phenomena. For this model we have used the correlations published by Shah for condensation [29] and evaporation [28], that show good prediction capacity and wide range of applicability.

For the condensation process, the Shah correlation for heat transfer in the turbulent regime flux has the following form:

$$h_i = h_{LT} \cdot \left(\frac{\mu_f}{14 \cdot \mu_g}\right)^{0.0058+0.557\cdot p_r} \left[(1-x)^{0.8} + \frac{3.8\, x^{0.76} \cdot (1-x)^{0.04}}{p_r{}^{0.38}}\right]$$

Where μ_l and μ_g are the viscosities of the liquid and gas phase respectively, p_r is the condenser reduced pressure, x is the quality and h_{LT} is the heat transfer coefficient if all the flow was flowing in the liquid state fluid phase, calculated as

$$h_{LT} = 0.023 \cdot Re^{0.8} \cdot Pr^{0.4}$$

Which is the Dittus-Boelter correlation, where Re is the Reynolds number and Pr is the Prandtl number, that are calculated according to

$$Re = \frac{4\dot{m}}{\pi \cdot d_i \cdot \mu} = \frac{G \cdot d_i}{\mu}$$

$$Pr = \frac{\mu \cdot C_p}{\lambda}$$

Where m is the pipe mass flow, d_i the pipe inner diameter, μ is the refrigerant viscosity, C_p is the refrigerant heat capacity and λ is the refrigerant thermal conductivity. G is the total mass flux in the pipe and is just the mass flow divided by the pipe cross-sectional area, but is introduced here since it will be referred later to explicitly indicate the strong dependency of the heat transfer coefficient with the mass flow rate.

For the evaporator, the Shah correlation consists of 5 different equations, among which the one with the highest value at the current conditions is selected. See [28] to get the details of the implementation of the correlations. Both expressions are evaluated in the model for a quality = 0.6, that returns a value close to the average value of the function.

The model also includes the calculation of the internal heat transfer coefficient during single-phase flow by the Gnielinski approximation, since in small sections of the HX pipes there is a single-phase flow. The resulting heat transfer can be calculated as a weighted average of the corresponding phase flows, but in the current model the heat transfer is set equal to the two-phase flow heat transfer, since this is the dominant regime.

The model of PCM storage (see 4.3.3) is a lumped capacitance model, which means that the storage is represented by a single temperature value. This strongly overestimates the resulting heat transfer since this approximation does not represent the temperature gradient developed inside the solid body of the storage when the Biot number is greater than 1. The Biot number is defined by the ratio of the external convective heat transfer (the refrigerant convection previously calculated) and the conductivity heat transfer which is relatively low in most PCM materials [30]. For the CHEST application modelled, the Biot number is in the range of 100, meaning that there is a significant thermal resistance to the heat transfer from the HX pipe towards the interior of the PCM material.

To take this into account on the overall energy balance of the system, it is possible to use a correction on the heat transfer that allows the lumped capacitance model to hold under situations with large Biot number [31], [24]. In short, the lumped capacity can be used for large Biot number systems by substituting the heat transfer by an effective heat transfer. This correction depends on the geometry of the system, but for our geometry (see Figure 9) is:

$$h_{eff} = \frac{1}{\frac{1}{h} + \frac{1}{\lambda} \cdot \frac{a^3(4b^2 - a^2) + ab^4\left(4Ln\left({}^{b}/_{a} - 3\right)\right)}{4(b^2 - a^2)^2}}$$

Where h is the heat transfer calculated as previously described, λ is the PCM conductivity and b and a are the external and internal radius of the single pipe PCM cell. This correction is used to incorporate the PCM resistance to the heat transfer process.

The conductivity is affected by the PCM convection when the material is melted. The PCM convection is calculated as the free convection around a cylinder due to density gradients in the medium surrounding the pipe. In this situation, the Nusselt number can be approximated by [25]:

$$Nu = \left[0.6 + \frac{0.387 \cdot Ra^{1/6}}{\left[1 + \left({}^{0.559}/_{Pr}\right)^{9/16}\right]^{8/27}}\right]^2$$

Where Pr is the Prandtl number and Ra is the Rayleigh number, evaluated with a surface temperature equal to the refrigerant condensing temperature. The Nusselt number relates with the heat transfer coefficient like

$$h = \frac{\lambda \cdot Nu}{d}$$

where d is the pipe outer diameter. The resulting convective heat transfer inside the PCM is them included in the effective heat transfer equation as an additive term to the PCM conductivity, using as a characteristic length a quadratic function of the melt fraction of the store between the single tube PCM cell inner and outer diameter.

Finally, to account for the effect of finned pipes in the model, a multiplicative to the heat transfer is included. Since the topic of heat transfer enhancement techniques for PCM is still an open topic [32], this multiplicative factor could serve well to incorporate the effect of other enhancement techniques in a simplified way. In our model, focused on the concept of large-scale energy storage, we will consider fins since it is a non-expensive solution available in the market and more predictable to evaluate in terms of cost. For our model, we chose a value of 30 % increase based on experimental data from [33], but this is just a gross approximation that can be edited manually by the user with any other value.

In the figure 10, the heat transfer coefficient is shown, for the case of butene as refrigerant and nitrate salts as PCM material when the PCM is in solid phase is shown in the next figure for several values of the HX pipe diameter:

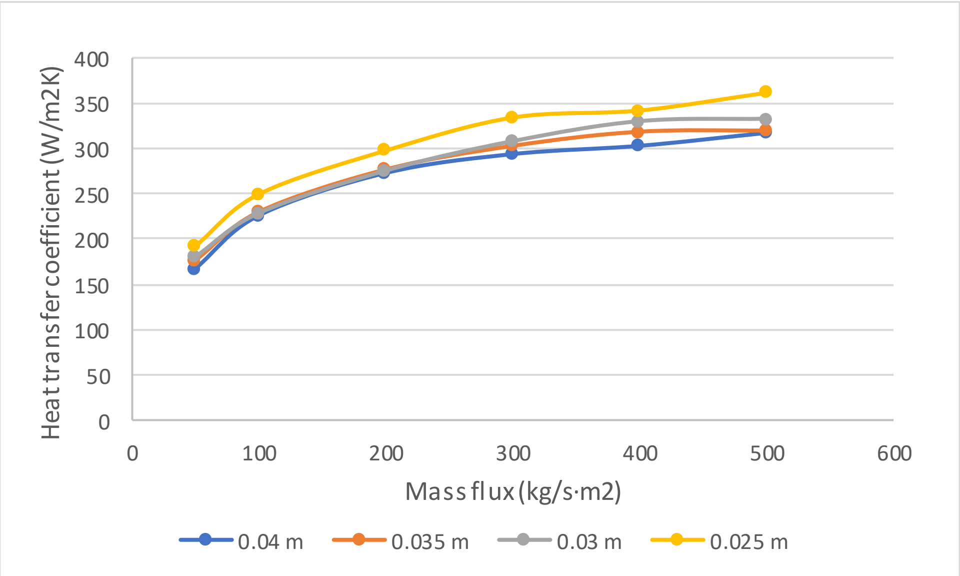

Figure 10: Overall heat transfer coefficient

It is worth to mention that experimental literature results for the overall heat transfer coefficient for condensation heat transfer in PCM have not been found, so a solid comparison is not possible. However, due to the low characteristic conductivity, the PCM resistance is the governing process in the heat transfer dynamics, so comparison with published data for other fluids can give a basis for comparison with the obtained results.

For example, in Esteves et al. [34], experimental data for the overall heat transfer coefficient for two different PCM with thermal oil as heat transfer fluid is presented. Values shown are mostly between 100 and 1000 W/m²·K, with some data reaching up to 1800 W/m²·K. Colella et al. [35], present data for the average heat transfer for a Paraffin based PCM (melting temperature of 100 C) with water as heat transfer fluid, and the resulting values are in the range from 150-600 W/m²·K. In Izquierdo et al. [36], an experimental study of different PCM heat exchangers, one of them with identical geometry as the one simulated here, is presented. Resulting overall heat transfer coefficients are in the range of 10 to 140 W/m²·K. Bashar [37], also presents experimental data for the heat transfer coefficient of PCM under different charging/discharging conditions, with resulting values of the overall heat transfer coefficient in the range of 200- 300 W/m²·K. In general, the available published literature with experimental data of heat transfer coefficient of PCM materials show the following trends:

- Values ranging from 100 to 1000 W/m²·K
- Heat transfer coefficient increasing with increased PCM melt fraction
- Heat transfer coefficient increasing with increasing heat transfer medium flow rate
- Increased heat transfer coefficient with increasing temperature difference between PCM and heat transfer medium
- Thermal heat transfer dominated by the PCM conductivity
- Increased heat transfer coefficient discharging than while charging

All these characteristics are reproduced by the model developed by Aiguasol for T4.2, so although the inherent uncertainty of the heat transfer phenomena during condensation/evaporation [29] [28], we consider that the model properly reproduces the dynamics of the system in this

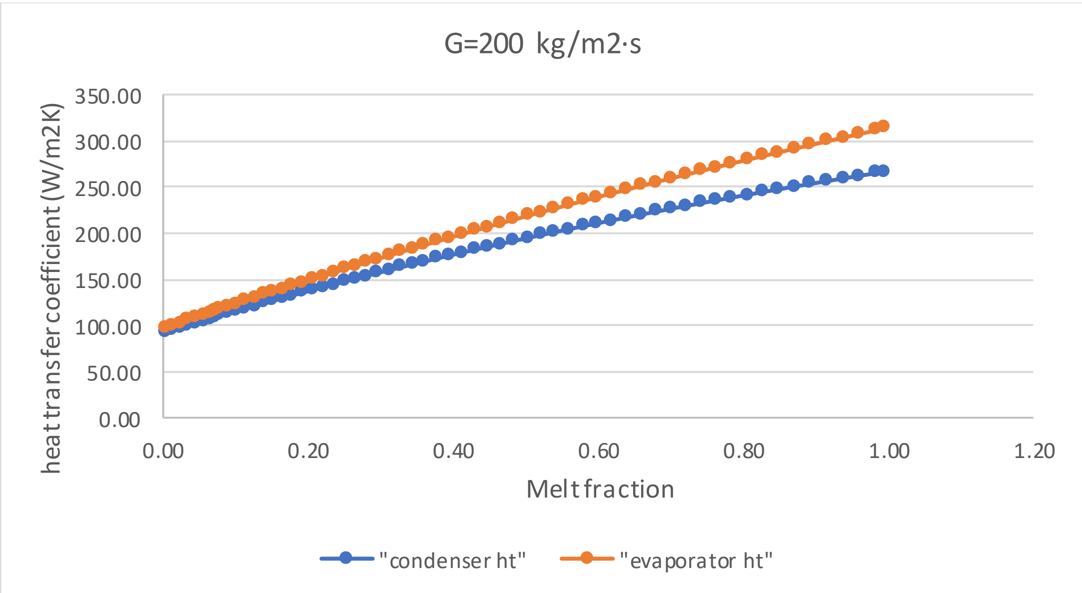

Figure 11: Heat transfer coefficient during condensation/evaporation as a function of the PCM melt fraction. Refrigerant: butemne, PCM: Litium salts, mass flux= 200 kg/m²·s, pipe inner diameter=0.025 m

According to the result of the heat transfer coefficient, we will need a high mass flux inside the pipe tubes, over 200 kg/(s m²) to have a good value of the heat transfer coefficient. This has implications in the geometry of the PCM storage, since the mass flux is a function of the compressor mass flow, the number of pipes in the heat exchanger and the pipe diameter. This will be used later as a criterion to size the CHEST model system, and will help evaluate the required temperature difference between the PCM storage material temperature and the refrigerant condensing temperature.

4.7.2. Model control

The model of the system has two levels of control. The first is the overall control of the system, which establishes if the system is charging electricity, discharging it or is idle. The model uses two external signals, one to set if there is demand from the net to charge and another for discharge, and this will be the input given by the optimizer to be developed in the T4.4. In the current status of the model, this is an input read from an external file, that has been generated in a simplified way from the data of the electricity market of Spain for 2018.

Whenever there is an external demand from the net, the system is ON if there are two more conditions met:

1. That the PCM storage is available to charge/discharge
2. That the SHS is available to charge/discharge

If the three conditions are met, then the model evaluates the mass flow rate of refrigerant and the condensing temperature of the HP (while charging) and the evaporating temperature of the ORC (while discharging) using two equations.

Here, we are referring to condensing temperature, which is the relevant one while charging the CHEST, but the calculation of the ORC evaporation temperature is analogous to this description. First, the heat released at the condenser has to fulfill:

$$Q_{condenser} = h \cdot A \cdot (T_{condensing} - T_{PCM})$$

Where h stands for the heat transfer coefficient at the condenser, A is the area of the condenser and $T_{condensing}$ is the current condensing temperature and T_{PCM} is the temperature at the PCM storage. The second equation used is

$$Q_{condenser} = \dot{m} \cdot \Delta h$$

Equating these two expressions, we have a relationship between the condensing temperature and the refrigerant mass flow rate through the HP loop (which is assumed constant for all the components). The heat transfer coefficient is calculated according to the procedure described in section 4.7.1, the area of the heat exchanger is defined based on the user inputs and the enthalpy difference through the condenser is calculated based on CoolProp information. The flow rate is an output from the compressor model (based on the current time step electricity consumption) and this allows to calculate the condensing temperature for the current system conditions. The process is solved iteratively, since the compressor mass flow rate is calculated based on the input of condensing temperature (see section 4.4.1).

This approach means that the HP condensing temperature/ORC evaporation temperature is variable during the system operation, while the electricity absorbed/generated is constant. This will have implications on the system performance due to the reduced COP of the heat pump associated to increase the discharge pressure, but is the only realistic mechanism found so far.

4.7.3. Model use and system sizing

The use of the model has been simplified by the inclusion of several equation blocks in the upper part of the simulation environment. There are three equation blocks called “Inputs”, “Parameters” and “Sizing”. Based on the information from this data, the model correlates the rest of the system properties, greatly simplifying the system use. For example, setting the HP power in the inputs equation block the model evaluates the required area of the PCM condenser, ensuring that the simulation parameters are consistent. Also, based on the HP and the ORC power the SHS is sized in terms of required energy, volume and dimensions (which are used to evaluate, for instance, the thermal losses coefficient of the storage).

The parameters in this equation blocks are described in the simulation environment, including the units of the parameter.

To calculate the sizing of the system, an Excel sheet has been produced, that helps on defining the inputs to the system. The motivation is that some previous iteration is necessary when sizing the condenser/evaporator of the PCM, since the estimated heat transfer coefficient is a function of the mass flux and this in time depends on the geometry of the PCM storage. Here we give a short description of the process to point the implications of the calculated effective heat transfer on the temperature difference between refrigerant condensing temperature and melting temperature.

The given sizing procedure uses as starting point the HP power and the ORC power, which are defined by the user in the Inputs equation block; from this, the HX area of the PCM is calculated as the maximum value of the next two expressions. The first is the required power of the PCM condenser, evaluated as

$$P_{cond,PCM} = P_{HP} \cdot Ratio_{LS} \cdot COP_{HP}$$

Where P_{HP} is the heat pump power, the $Ratio_{LS}$ is the ratio of latent heat expected (based on HP cycle) and COP_{HP} is the heat pump estimated COP. The second is

$$P_{evap,PCM} = P_{ORC} \cdot Ratio_{LS} / \eta_{turbine}$$

With this, the PCM HX area is calculated as:

$$Area_{HX,PCM} = \max\left(P_{cond,PCM}, P_{evap,PCM}\right) \Big/ \left(h_{eff} \cdot \Delta T\right)$$

Where the delta T is the temperature difference between condensing/evaporator temperature and the melting temperature and h_{eff} has to be guessed since the mass flow of a single pipe is still unknown (we do know the total mass flow, but not the number of pipes).

The calculated HX area is used to determine the total length of the HX, using the diameter of the pipes as a user defined input. The total length of pipes is calculated with

$$Area_{HX,PCM} = 4\pi {d_i}^2 L_{HX,PCM}$$

With the total length of pipes is known, we have already set the storage capacity, since the thickness of the PCM material surrounding the pipe is defined. Due to the impact in the effective heat transfer calculation, it is not recommendable to increase this quantity so much. For the current design, a ratio of 0.005 m^3 per unit length of pipe is considered (this, as all the parameters used for system sizing can be edited in the equation block “Sizing”), so the storage volume is

$$Vol_{PCM} = Ratio_{PCM\ to\ HX} \cdot L_{HX,PCM}$$

Then the storage energy is

$$Q_{PCM} = Vol_{PCM} \cdot \rho_{PCM} \cdot \Delta H_{PCM}$$

Which is the product of the volume, density and PCM phase change enthalpy.

The charging and discharging time can be calculated as

$$t_{charge} = {Q_{PCM}}/{P_{HP}}$$

$$t_{discharge} = {Q_{PCM}}/{P_{ORC}}$$

To calculate the pipe length, we want to ensure that the aspect ratio of the storage is kept in reasonable values. The aspect ratio is defined here as the height of the storage divided by the base area, and we use by default of 3. Longer pipes are beneficial, but they set also the height of the storage, and cannot be increased arbitrarily due to hydraulic and stability reasons, so we assume a maximum value of 10 meters. So, the pipe length is calculated as

$$L_{pipe} = \min\left(10, AspectRatio \cdot \sqrt[3]{Vol_{PCM}}\right)$$

And the total number of pipes is

$$N_{pipes} = {L_{HX,PCM}}/{L_{pipe}}$$

The total mass flow can be estimated as

$$\dot{m}_{cond} = {P_{cond}}/{\Delta H_{refrigerant}}$$

$$\dot{m}_{evap} = {P_{evap}}/{\Delta H_{refrigerant}}$$

And the mass flux is

$$G = \frac{4 \cdot \dot{m}}{\pi \cdot d_i^2}$$

We can calculate the size of the system as an example for some standard conditions. For a 1000 kW heat pump and 500 kW ORC turbine, we assume a pipe diameter of 0.025 m, a heat transfer coefficient of 300 W/m_2.K, COP of 3, turbine efficiency of 0.15, a ratio of latent heat of 0.6 and temperature difference of 5 K between refrigerant and PCM, we get the following results

$$Area_{HX,PCM} = \max\left(P_{cond,PCM}, P_{evap,PCM}\right) \cdot h_{eff} \cdot \Delta T = 1333.3\, m^2$$

$$L_{HX,PCM} = {Area_{HX,PCM}}/{4\pi \cdot d_i {d_i}^2} = 16976\ m$$

$$Vol_{PCM} = Ratio_{PCM\ to\ HX} \cdot L_{HX,PCM} = 84.9\ m^3$$

$$Q_{PCM} = Vol_{PCM} \cdot \rho_{PCM} \cdot \Delta H_{PCM} = 7.5\ MWh$$

$$L_{pipe} = \min\left(10, AspectRatio \cdot \sqrt[3]{Vol_{PCM}}\right) = 10\ m$$

$$N_{pipes} = {L_{HX,PCM}}/{L_{pipe}} = 1698\ tubes$$

Evaluating the mass flux, we get

$$G = \frac{4 \cdot \dot{m}}{\pi \cdot d_i^2} = 18.6\ {kg}/{m^2 \cdot s}$$

Going back to the heat transfer coefficient as a function of the mass flux:

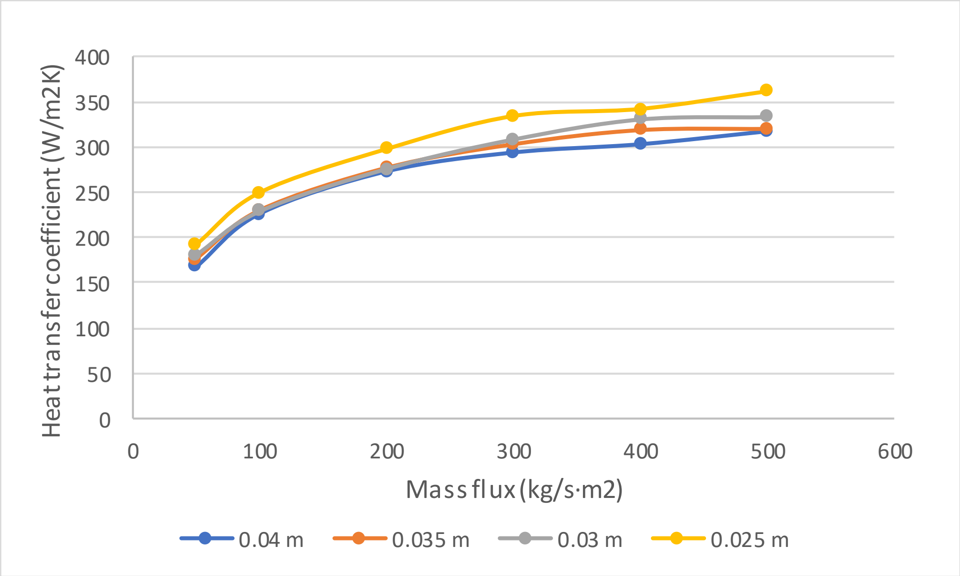

Figure 12: Overall heat transfer coefficient

We can see that our initial hypothesis of heat transfer coefficient of 300 W/(m^2·K) is not fulfilled. In fact, the value of 18 we just found yields a heat transfer coefficient under 100 W/(m^2·K).

To alleviate this, we can do two things, increase the heat exchanger area or increase the temperature difference between condensing and melting temperature. Increasing the surface area is not advisable, since an area increase means that we increase the number of tubes, hence the mass flux will be reduced and the heat transfer will drop. Thus, the only option available is to increase the temperature difference. In the previous example, we can solve for the temperature and we find that the required temperature difference reaches 53 K. Reducing the diameter to 0.02 m will keep the temperature difference just in 40 K.

Besides the number examples, which shall be considered just a roughly estimation of the real sizing, it is apparent from the system sizing that the heat transfer coefficient of the system together with the small temperature differences considered so far are not compatible, since they impose an excessive area of heat exchanger, that penalizes the heat transfer due to the low mass flux. In the future, when the system is operated with the case studies, we will address this issue by searching new combinations of PCM material and refrigerant that better match the system requirements.

The need of adapting the PCM material and refrigerants to each case study is even more evident if we consider the close relation of the district heating temperature and HP heat source temperature in the performance of the overall system. For the case of Ispaster, the heat source for the evaporator is the solar thermal energy, while for the case of Aalborg this heat should come from residual waste heat. This has implications in three system parameters which are very relevant for system sizing: latent to sensible heat ratio, heat pump COP and ORC turbine efficiency.

To maximize the system performance, we would need to maximize the heat pump COP, the turbine efficiency and the latent to sensible ratio of the system. Moreover, it is necessary to keep the latent fraction of the HP condenser and the ORC evaporator as close as possible, in order to reduce the SHS size, hence also the investment associated and the thermal losses. The following figure shows the heat pump COP working with butene and a condensing temperature of 138 C as a function of the evaporator temperature. The different lines in the graph represent variable values of the LTWT temperature:

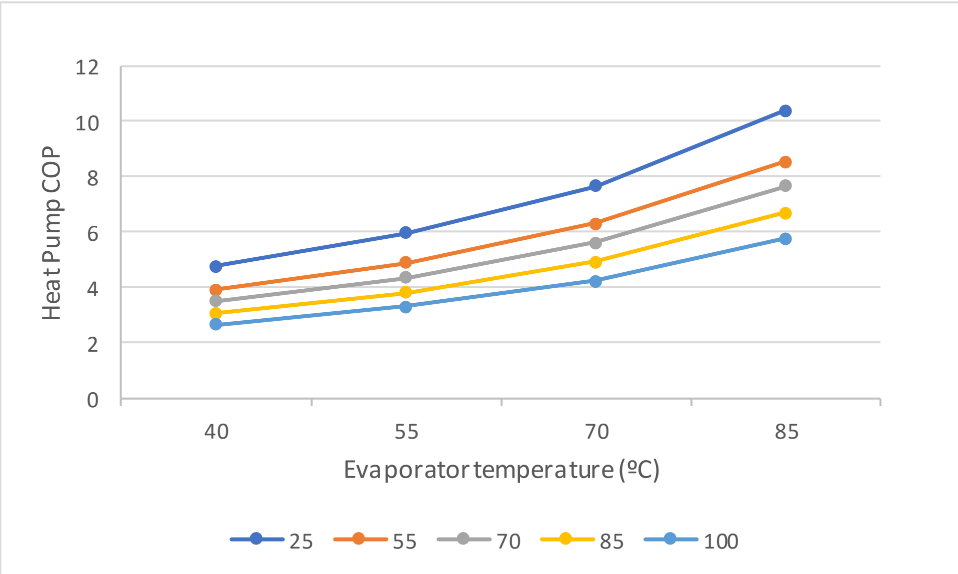

Figure 13: Heat pump COP for different LTWT temperature

As expected, the COP increases with growing evaporation temperature and lower SHS temperature. However, the amount of electricity stored in the PCM in form of heat for a unit of electricity consumed by the heat pump is the product of the COP in the previous graph by the latent ratio of the thermal energy generated, as shown in the following graph:

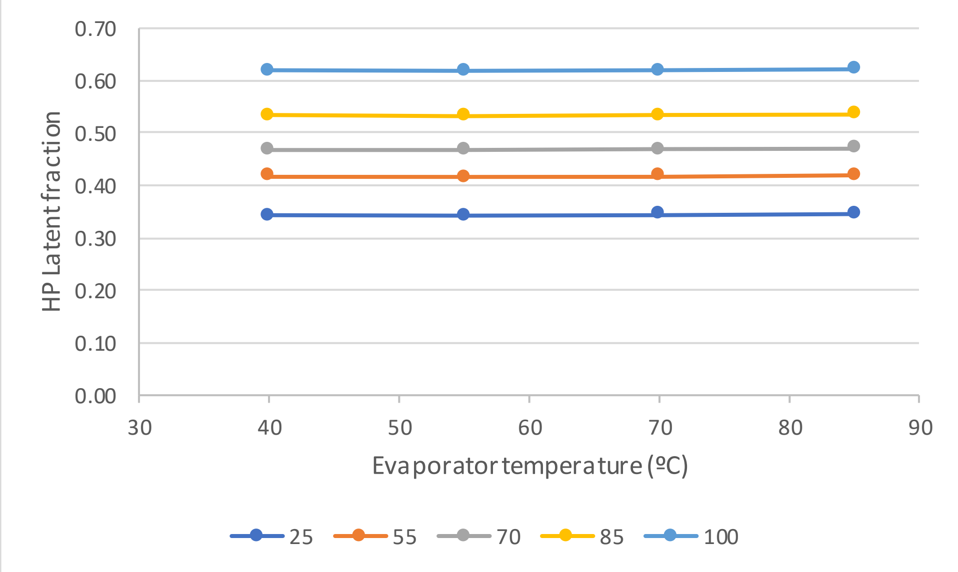

Figure 14: Latent fraction of heat by the HP for different LTWT temperature

Here, we would also like to maximize this quantity, since the amount of recoverable heat from the PCM is proportional to the latent fraction, but as seen in the figure 13, the latent ratio grows with increasing temperature at the SHS, which as shown in figure 12, penalizes the COP. An optimum should be found that will depend on the refrigerant properties.

A similar consideration can be done for the ORC turbine, although in this case, the LTWT has no effect in the turbine efficiency, and instead of the evaporator temperature, the condensing temperature is the relevant parameter for determining efficiency. The figure 14 shows the dependency of the ORC turbine with condensing temperature for butene as working fluid and an evaporator temperature of 128 C:

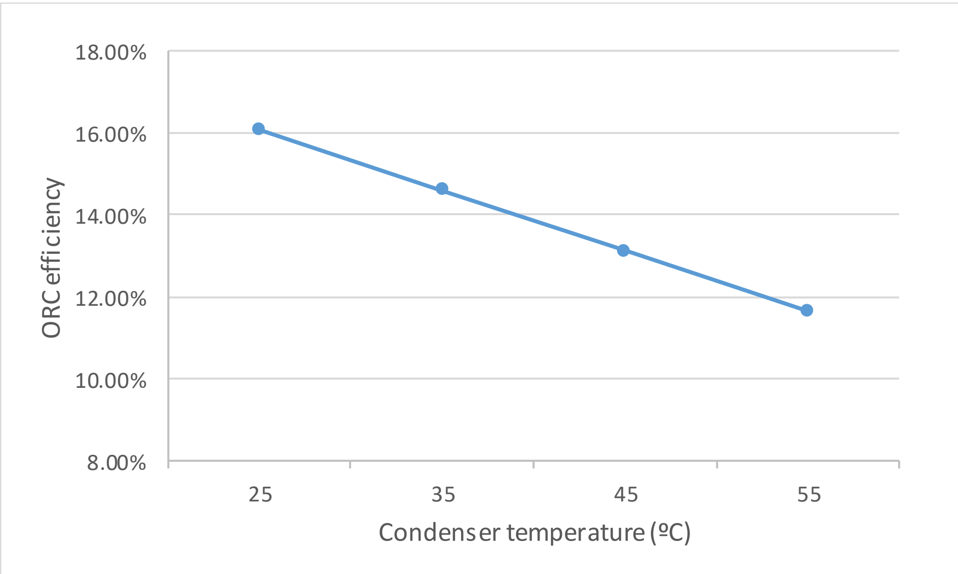

Figure 15: ORC efficiency as a function of condenser temperature

In this case, the efficiency is not dependent on the temperature of the LTWT so there is a unique curve instead of different ones as happened with the COP of the heat pump. However, the ratio of latent heat to total heat for the ORC loop is affected by the LTWT temperature as shown in figure 15:

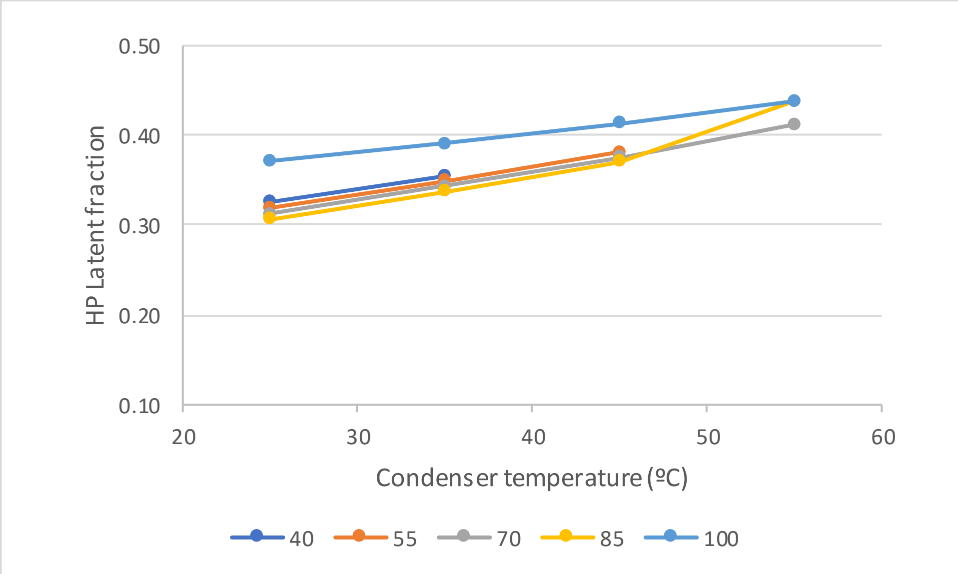

Figure 16: Latent heat ratio of ORC loop for different LTWT temperatures

As previously said, it is favourable to have similar latent power at the different loops. Comparing this figure with the figure 13, where the HP loop latent ratio is presented, we find that in the HP loop this quantity has more variability than for the ORC loop, and reaches higher values, which is preferably for the electricity storage operation. A different power sizing for the ORC and heat pump capacity can help to match these quantities since the ratio has to be multiplied by the loop electrical capacity to get the SHS power released. However, for a system with equal capacity in both loops with this PCM material will benefit from having a LTWT temperature between 55 and 70 C, since this would equalize the sensible heat release generated at both loops.

4.8. Model outputs

The model results are collected in two Excel spreadsheet files for each simulation, one called "Energy_bal.xls" and the other "Econ_bal.xls". They have integrated values in monthly basis for different energetic and economic results of the system, as well as the maximum and minimum integrated and instantaneous values. The results can be grouped in three categories:

1. Energy outputs: they show the integrated quantities for several energy flows in the system: storage losses, electricity generated by the turbine, electricity consumption by pumps…All energy outputs are in kJ/h.
2. Economic outputs: integrated quantities for economic flows: income from selling electricity, electricity costs for pumping, income from district heating generated heat…the price of district heating, waste heat or other prices can be set at the

"Economic" equation block in the model, while the electricity price is variable in hourly basis and read from an external file. All economic outputs are in €.

3. Availability outputs: hours of operation of the system, hours of grid demand, hours lost for fully charged or discharged storage…they are used mainly as a help for properly size the system. All availability outputs have units of time (hours).

Table 3 shows a list of the outputs, for the file "Energy_bal.xls", indicating the header and a description of the output:

Table 3: List of model results at the Energy_bal output file

Result header	Description
CMP_Consum	Electricity consumption by the compresor
CMP_ThLs	Thermal losses at the compresor
CMP_EleLs	Electrical losses at the compresor motor
CMP_Wfluid	Compresor useful work on the fluid
PCM_CondGain	Heat gain at the PCM from the heat pump
PCM_EvapGain	Heat delivered by the PCM to the ORC
PCM_ThLs	Thermal losses at the PCM storage
SBC_ht	Heat transfer at the HP subcooler
HP_Evap_ht	Heat transfer at the HP evaporator
HTWT_Gain	Energy gain at the HTWT storage
LTWT_Gain	Energy gain at the LTWT storage
HTWT_Th_Ls	Thermal losses at the HTWT
LTWT_Th_Ls	Thermal losses at the LTWT
HTWT_Aux	Auxiliary consumption needed for compensate thermal losses at the HTWT
LTWT_Aux	Auxiliary consumption needed for compensate thermal losses at the LTWT
Pu_Ch_WrEle	Electricity consumption by the SHS pumping while charging
Pu_Ch_Wrfluid	Heat transfer to fluid by the SHS pumping while charging
Pu_DCh_WrEle	Electricity consumption by the SHS pumping while discharging
Pu_DCh_Wrfluid	Heat transfer to fluid by the SHS pumping while discharging
Pu_cnd_WrEle	Electricity consumption by the ORC loop condensate pump
Pu_cnd_Wrfluid	Heat transfer to fluid by the ORC loop condensate pump
ORC_gross_pow	ORC gross electricity production
ORC_net_pow	ORC net electricity production
ORC_cnd_ht	Heat transfer at the ORC loop condenser
ORC_preh_ht	Heat transfer at the ORC loop preheater
WH_cons_evap	Waste heat consumption at the evaporator
Ax_cons_evap	Auxiliary consumption at the evaporator
WH_cons_SHS	Waste heat consumption for compensating SHS thermal losses
Ax_SHS_Th_Ls	Auxiliary consumption for compensating SHS thermal losses
WH_Exces	Excess waste heat available
DH_useful_energy	Useful energy delivered to the district heating network
DH_Load	Load required by the district heating network
U_PCM	Temperature of the PCM storage (non integrated, this is an end of month value)

U_LTWT	Internal energy change at the LTWT (non integrated, this is an end of month value)
U_HTWT	Internal energy change at the HTWT (non integrated, this is an end of month value)

For the econ_bal.xls file, the list of outputs is shown in table 4:

Table 4: List of model results at the Econ_bal output file

Result header	Description
ORC_gross	ORC gross electricity production
ORC_net	ORC net electricity production
ORC_Ele_sell	Income from electricity sold
HP_consumption	Electricity consumption by the compresor
HP_Ele_cost	Cost of the electricity from the HP operation
HP_Pr_Ele	Parasitic electricity consumption while charging
HP_Pr_cost	Cost of the electricity from the parasitic consumptions while charging
GAS_SHS	Gas consumption for compensating the SHS
GAS_HP_Evap	Gas consumption at the HP evaporator
GAS_cons	Total gas consumption
SHS_Gas_cost	Cost of gas for compensating the SHS
EV_Gas_cost	Cost of gas used at the HP evaporator
Ele_balance	Sum of all the electricity flows incomes and expenses
Gas_balance	Sum of all the gas flows expenses
Economic_balance	Sum of all the incomes and expenses
EV_WH	Waste heat consumption at the HP evaporator
EV_WH_cost	Cost of the waste heat consumption at the HP evaporator
SHS_WH	Waste heat consumption at the SHS
SHS_WH_cost	Cost of the waste heat consumption at the SHS
WH_cost	Total waste heat costs
DH_sold	Energy sold to the district heating network
DH_income	Income from the energy sold to the district heating network
Discharge_time	Total operating time discharging
Grid_DCh_time	Hours with discharge demand from the grid
PCM_DCh_Full_time	Hours of discharge lost due to an empty PCM storage
SHS_DCh_Full_time	Hours of discharge lost due to an empty SHS storage
DH_DCh_Av	Hours of discharge with demand at the district heating network
Charge_time	Total operating time charging
Grid_Ch_time	Hours with charge demand from the grid
PCM_Ch_Full_time	Hours of charge lost due to a full PCM storage
SHS_Ch_Full_time	Hours of charge lost due to a full SHS storage
WH_Av	Hours with availability of waste heat

5. Conclusions

The work done in the task 4.2 yields several relevant output and conclusions for the future development of the CHETSER project. To start, one of the outputs of the task is a dynamic model of the CHEST system coupled to the energy system that can be used to evaluate the performance of the system under a great variety of situations (for instance the selected two case studies, Ispaster and Aalborg, as it will be done in T4.3). This includes also the modification of the refrigerant or PCM material, which is a necessary step towards the optimization to be carried in T4.3, (Full scale optimized CHEST system development). Also, a set of TRNSYS types have been generated specifically to model the CHEST system, and they by themselves can be used also in other tasks in the project if necessary.

Besides these specific outputs, that are expected to be the core of the T4.4 management system, it has been reached two conclusions for the CHEST system design, regarding technical and exploitation aspects, that have several implications on the system development.

First conclusion, regarding the exploitation of CHEST, an operation on multiple sequential markets is the recommended approach to maximize the revenues from the exploitation of grid services, as has been already proposed for the participation of other electrical storage devices. This means that CHEST should operate in the DAM, as well as in as many as possible balancing markets. This has several implications:

- Given the short reaction time upon request characteristic of the balancing markets, in order to deliver grid services with due quality, a steady and constant electrical input and output must be maintained. In other words, the heat pump electricity consumption and expander electrical generation should be kept constant when the system is operating. This is a fundamental change in the classical operation of heat pump systems, since those are usually driven by a heat demand and a variable electrical input is used to cope with the demand. If the CHEST system is going to provide grid services, the heat pump control should adapt to follow grid requirements.
- So far, the CHEST system could operate on two electrical markets simultaneously (DAM and RR markets), according to the expected prize evolution at each of them and this duplicity enhances the opportunities to operate. However, the participation in several markets means that some technical conditions have to be fulfilled that put additional constraints on the system design. In particular, a minimum capacity is required to participate in the RR market, so CHEST will have to meet these criteria which is currently diverse among European countries, but we estimate that the ongoing market standardization at European level, [1] will leave this value around 1 MW. Due to this, we believe that a good reference for system size at initial stages of development could be 1 MW.
- The ability to participate in other balancing markets (aFRR, mFRR) is limited by the start-up time of the turbine and the heat pump. If the system evolves towards a faster response time, more and better chances to provide grid services will appear. Another way to address this limitation on the response time would be the hybridization of the CHEST with a small capacity battery system.

A second conclusion, is the relatively poor performance of the PCM storage when compared with conventional condenser and evaporators. This is a frequent topic in the PCM scientific literature [32] [33] [30] [34] and the implications arise when analysing the model outputs. This bad performance is originated by the low conductivity of PCM materials, and in terms of system design and operation has several implications:

- The low conductivity by the PCM limits the heat transfer in the heat pump condenser. Since, as we mentioned before, the electrical input must be kept constant, the only way to maintain the heat transfer to the PCM is to increase the temperature difference between the compressor discharge temperature and the PCM melting temperature. This can be especially critical when the PCM is in fully solid state, since the lack of convection inside the storage worsen the situation
- Due to this a higher temperature difference among the working fluids (refrigerant and PCM) has to be maintained than in conventional applications (5-10 K). This means that in order to avoid the refrigerant reaching his critical temperature (what poses additional problems), a minimum temperature difference between the refrigerant critical temperature and the PCM melting temperature is necessary. There isn't a single figure to recommend since this is strongly dependent on many geometrical parameters of the PCM and thermophysical properties of the materials. This limits the potential of using some of the pairs considered on the literature, as the combination of Butene with some Li salts, since their respective critical temperature and melting temperature are too close.
- Besides this effect on material selection, this high pinch point will have a negative effect on the HP COP and the ORC efficiency, so it has to be managed carefully. To address the problem, the most adequate way is to analyse new materials for the PCM and working fluids, so this will be one of the key optimization parameters in T4.4. In general, a review of the PCM/refrigerant pairs should be done in the light of the work presented in this document, considering a higher temperature difference between them in the PCM storage and the need of having a higher difference between melting and critical temperatures.

References

[1] ENTSOE, «AN OVERVIEW OF THE EUROPEAN BALANCING MARKET,» 2018.

[2] ECA, «EU support for energy storage,» 2019.

[3] D. Energy, «The future role and challenges of Energy Storage».

[4] EASAC, «Valuing dedicated storage in electricity grids,» 2017.

[5] S. N. Laboratories, «Energy Storage for the Electricity Grid: Benefits and Market Potential Assessment Guide,» 2010.

[6] Comission Staff Working Document, *Energy storage-the role of electricity,* 2017.

[7] E. Parliament, «EUR_Lex,» 5 June 2019. [Online]. Available: https://eur-lex.europa.eu/legal-content/EN/TXT/?uri=CELEX:32019L0944. [Consultato il giorno September 2019].

[8] IRENA, «Renewables and electricity storage,» 2015.

[9] E. Barbour, I. Grant Wilson, J. Radcliffe, Y. Ding e Y. Li, «A review of pumped hydro energy storage development in significant international electricity markets,» *Renewable and Sustainable Energy Reviews,* n. 61, pp. 421-432, 2016.

[10] International Electrotechnical Commission, «Electrical Energy Storage,» 2011.

[11] D. Conolly, H. Lund, P. Finn, B. Mathiesen e M. Leahy, «Practical operation strategies for pumped hydroelectric energy storage(PHES) utilising electricity price arbitrage,» *Energy Policy,* n. 39, pp. 4189-4196, 2011.

[12] R. Deb, «Operating hydroelectric plants and pumped storage units in a competitive environment,» *The electricity journal,* vol. 13, n. 3, pp. 24-32, 2000.

[13] A. Ugedo, E. Lobato, A. Franco, L. Rouco, J. Fernandez e J. Chofre, «Validation of a strategic bidding model within the Spanish sequential electricity market,» in *EEE 11th International Conference on Probabilistic Methods Applied to Power Systems*, 2010.

[14] J. Perez-Diaz, «Trends in the operation of PHS,» in *5th Workshop on Hydro Scheduling in Competitive Electricity Markets*, 2015.

[15] EUR-Lex, «https://eur-lex.europa.eu,» 27 November 2017. [Online]. Available: https://eur-lex.europa.eu.

[16] European University Institute, «Introduction to network tariffs and network codes for consumers, prosumers and energy communities,» 2018.

[17] SmartEn, «SmartEn Map: European balancing markets,» 2018.

[18] Energinet, «https://energinet.dk,» [Online]. Available: https://energinet.dk/-/media/Energinet/El-RGD/El-CPL/Dokumenter/Udbudbetingelser/Systemydelser-til-levering-i-Danmark---Udbudsbetingelser.pdf . [Consultato il giorno 15 11 2019].

[19] Solar Energy Research Laboratory, University of Madison-Wisconsin, «http://sel.me.wisc.edu/trnsys».

[20] Bell Thermal Consultants, «www.coolprop.org».

[21] H. Jockenhöfer, W.-D. Steinmann e D. Bauer, «Detailed numerical investigation of a pumped thermal energy storage,» *Energy,* n. 145, pp. 665-676, 2018.

[22] P. Vinnemeier, M. Wirsum, D. Malpiece e R. Bove, «Integration of heat pumps into thermal plants for creation of large-scale,» *Applied Energy,* n. 184, pp. 506-522, 2016.

[23] A. Smallbone, V. Jülch, R. Wardle e A. P. Roskilly, «Levelised Cost of Storage for Pumped Heat Energy Storage in comparison,» *Energy conversion and management,* n. 152, pp. 221-228, 2017.

[24] P. Li, B. Xu, J. Han e Y. Yang, «Verification of a model of thermal storage incorporated with an extended lumped capacitance method for various solid–fluid structural combinations,» *Solar Energy,* vol. 105, pp. 71-81, 2014.

[25] J. Lienhard, A heat transfer textbook, 4th Edition, Philogist Press, 2017.

[26] F. Incropera e D. DeWitt, Fundamentals of Heat and Mass Transfer., Hoboken,NJ: John Wiley & Sons, 2002.

[27] R. Santa, «The Analysis of Two-Phase Condensation Heat,» *Acta Polytechnica Hungarica,* vol. 9, n. 6, 2012.

[28] M. Shah, «Evaluation of General Correlations for Heat Transfer During,» in *ASME Heat Transfer Conference*, San Francisco, Californa, 2005.

[29] M. Shah, «An Improved and Extended General Correlationfor Heat Transfer During Condensationin Plain Tubes,» *HVAC&R Research,* vol. 15, n. 5, pp. 889-912, 2009.

[30] K. Reddy, V. Mudgal e T. Mallick, «Review of latent thermal energy storage for improved material stability and effective load management,» *Journal of Energy Storage,* n. 15, pp. 205-227, 2018.

[31] B. Xu, P.-W. Li e C. Lik Chan, «Extending the validity of lumped capacitance method for large,» *Solar Energy,* n. 86, pp. 1709-1724, 2012.

[32] B. Kanimozhi, A. Prabhu, M. Anish e P. Harish Kumar, «Review On Heat Transfer Enhancement Techniques in Thermal Energy Storage Systems,» *Int. Journal of Engineering Research and Applications,* vol. 4, n. 2, pp. 144-149, 2014.

[33] V. Thirunavukkarasu, S. Meyyapan e B. Gnanasikamani, «Experimental analysis of shell and tube thermal energy storage system with finned tube,» *Journal of Chemical and Pharmaceutical Sciences,* vol. 9, n. 4, pp. 3138-3141, 2016.

[34] EDSO, «Integrating electricity storage into distribution grids,» 2016.

[35] M. Chazarra, J. I. Perez-Diaz e J. Garcia-Gonzalez, «Optimal Joint Energy and Secondary Regulation Reserve Hourly Scheduling of Variable Speed Pumped Storage Hydropower Plants,» *IEEE Transactions on Power Systems,* 2017.